NASA TECHNICAL NOTE

NASA TN D-7801

NASA TN D-7801

EFFECTS OF VIBRATIONAL NONEQUILIBRIUM ON THE INVISCID DESIGN OF AN AXISYMMETRIC NOZZLE FOR HYPERSONIC FLOW

John B. Anders, Jr.

Langley Research Center

Hampton, Va. 23665

NATIONAL AERONAUTICS AND SPACE ADMINISTRATION • WASHINGTON, D. C. • JANUARY 1975

1. Report No.	2. Government Accession No.	3. Recipient's Catalog No.
NASA TN D-7801		

4. Title and Subtitle	5. Report Date
EFFECTS OF VIBRATIONAL NONEQUILIBRIUM ON THE INVISCID DESIGN OF AN AXISYMMETRIC NOZZLE FOR HYPERSONIC FLOW	January 1975
	6. Performing Organization Code

7. Author(s)	8. Performing Organization Report No.
John B. Anders, Jr.	L-9723
	10. Work Unit No.
	501-06-07-03

9. Performing Organization Name and Address	11. Contract or Grant No.
NASA Langley Research Center Hampton, Va. 23665	
	13. Type of Report and Period Covered
	Technical Note

12. Sponsoring Agency Name and Address	14. Sponsoring Agency Code
National Aeronautics and Space Administration Washington, D.C. 20546	

15. Supplementary Notes

16. Abstract

The design of an axisymmetric, hypersonic nozzle for arc-heated air is described. The method of characteristics is used to compute an inviscid nozzle contour in which vibrational nonequilibrium is approximated by the sudden-freeze technique. Chemical reactions are shown to freeze early in the nozzle expansion, and the result of vibrational and chemical freezing on the nozzle contour is demonstrated.

The approximate nozzle design is analyzed by an exact calculation based on the method of characteristics for flow with vibrational nonequilibrium. Exit profiles are computed, and the usefulness of the approximate design is discussed. An analysis of the nozzle performance at off-design conditions is presented.

17. Key Words (Suggested by Author(s))	18. Distribution Statement
Method of characteristics Hypersonic Nozzle	Unclassified – Unlimited STAR Category 12

19. Security Classif. (of this report)	20. Security Classif. (of this page)	21. No. of Pages	22. Price*
Unclassified	Unclassified	39	$3.75

*For sale by the National Technical Information Service, Springfield, Virginia 22151

EFFECTS OF VIBRATIONAL NONEQUILIBRIUM ON THE INVISCID DESIGN OF AN AXISYMMETRIC NOZZLE FOR HYPERSONIC FLOW

By John B. Anders, Jr.
Langley Research Center

SUMMARY

The design of an axisymmetric, hypersonic nozzle for arc-heated air with vibrational nonequilibrium is computed by the vibrational sudden-freeze technique. For stagnation conditions near the design values, calculations based on methods for quasi-one-dimensional flow indicate that the chemical composition of the gas (air) freezes very early in the expansion. The vibrational mode of the molecules freezes somewhat later in the expansion. A method-of-characteristics calculation for equilibrium air is used to design the supersonic, inviscid portion of a nozzle where vibration is "suddenly frozen;" that is, upstream of the freeze point vibration is in equilibrium, and downstream of the freeze point vibration is frozen.

This sudden-freeze nozzle is analyzed at design conditions by means of a characteristics calculation for frozen chemistry and vibrational nonequilibrium. The results of this analysis indicate that the approximate design provides reasonably uniform exit profiles at a Mach number about 3 percent lower than the design value of 9. The exit flow angularity is everywhere less than 0.1°, and the static-pressure variation across the exit is about 10 percent of the center-line value. Analysis of nozzle performance at slightly off-design stagnation conditions reveals no major deterioration of the flow quality.

INTRODUCTION

Wind-tunnel nozzle design has commanded considerable effort over past years when long and laborious method-of-characteristics (MOC) calculations were performed by hand. As higher Mach numbers were required, two-dimensional nozzles gave way to axisymmetric designs, and approximate methods such as that described in reference 1 were used. With the development of high-speed digital computers, numerous techniques using the MOC appeared (e.g., refs. 2 to 8). The high stagnation temperatures associated with high Mach number flight required calculations to account for real-gas effects (refs. 9 to 12) and for nonequilibrium (refs. 13 to 16).

In order to increase the flexibility and capability of the Langley 4-foot hypersonic arc tunnel described in reference 17, it was desirable to replace the existing high Mach number conical nozzle with a lower Mach number contoured nozzle. The present report develops the design for the new nozzle. The high temperature of arc-heated gas indicated that the nozzle design must be for a real gas with possible nonequilibrium.

One major difficulty facing the designer of a hypersonic wind-tunnel nozzle with nonequilibrium flow is that most available nonequilibrium MOC calculation schemes treat what is called the direct problem (nozzle contour is assumed given) instead of the indirect problem (nozzle contour is the unknown to be determined). For this reason an approximate design scheme was employed to generate the nozzle contour, and an existing direct MOC program modified to include some nonequilibrium effects was used to analyze the nozzle flow.

The existing tunnel complex placed many restrictions on the nozzle design. For example, both the arc heater and vacuum sphere limited the total mass flow of the system, and the operating characteristics of the arc heater limited the maximum practical stagnation pressure. The necessary trade-offs to optimize the design and the MOC calculations used to compute the contour are discussed. Vibrational nonequilibrium was treated in an approximate way, and the resulting nozzle design was analyzed by means of a direct vibrational-nonequilibrium MOC calculation. A boundary-layer correction to the inviscid contour was not computed for the nozzle, although such a correction could be quite large. Also, the subsonic-nozzle contour was not considered.

SYMBOLS

A	cross-sectional area
a	speed of sound
C_i	mass fraction of chemical species i
c_p	specific heat at constant pressure
$\bar{c}_{p,a}$	nondimensional specific heat, $c_{p,a}/c_{p,\infty}$
d	diameter
e_c	energy per unit mass in formation of chemical species, $\sum_i C_i h_{f,i}$

e_f	energy per unit mass frozen in vibration and/or chemical species
e_v	energy per unit mass in vibration
$\bar{e}_v$	nondimensional vibrational energy, $e_v/c_{p,\infty}T_\infty$
H	total enthalpy per unit mass
h	static enthalpy per unit mass
$\bar{h}$	nondimensional static enthalpy, $h/c_{p,\infty}T_\infty$
$h_{f,i}$	enthalpy of formation for chemical species i
i	index of chemical species
M	Mach number
$\dot{m}$	mass flow rate
n	coordinate normal to streamlines
p	pressure
$\bar{p}$	nondimensional pressure, $p/\rho_\infty u_\infty{}^2$
q	dynamic pressure, $\rho u^2/2$
R	universal gas constant
R_S	specific gas constant
R_∞	Reynolds number based on free-stream conditions at nozzle exit
r	radius
S	entropy per unit mass
s	coordinate along streamlines

$\bar{s}$	nondimensional coordinate, $\frac{s}{r^*}$
T	temperature
$\overline{T}$	nondimensional temperature, T_a/T_∞
t	time
U	velocity ratio, u/u_l
u	velocity
$\bar{u}$	nondimensional velocity, u/u_∞
u_l	limiting velocity
W	molecular weight of mixture
W_i	molecular weight of chemical species i
$\dot{w}_i$	chemical species production term
$\bar{\dot{w}}_i$	nondimensional chemical species production term, $\dot{w}_i r^*/\rho_\infty u_\infty$
x	coordinate along nozzle axis
$\bar{x}$	nondimensional axial coordinate, x/r^*
y	coordinate normal to nozzle axis
$\bar{y}$	nondimensional normal coordinate, y/r^*
γ	ratio of specific heats
η	characteristic variable
θ	flow angle
μ	Mach angle

ξ characteristic variable

ρ density

τ vibrational relaxation time

Subscripts:

a active degrees of freedom (translation and rotation)

i chemical species i

t stagnation condition

v vibration

1 arc-heated fluid

2 room-temperature fluid

3 arc-heated fluid mixed with room-temperature fluid

∞ free-stream conditions at nozzle exit

Superscript:

* throat of nozzle

DESIGN CONSIDERATIONS

Selection of Stagnation Conditions

Because of the high stagnation temperatures associated with arc-heated flows, most test models must be water cooled. In general, the models are therefore bulky and require a rather large test stream to avoid blockage. In view of this, the exit diameter of the nozzle was fixed at a minimum value of 15 cm. The exit Mach number was chosen to be 9 since the arc heater could duplicate the total temperature for flight at that Mach number.

For a real gas the area ratio required for a given Mach number is a function of the stagnation conditions. For heater operation at 100 atm (10.13 MN/m^2) the size requirement can be met by expansion to a free-stream Mach number of 9 for a mass flow of

approximately 0.27 kg/sec. Past experience with the present facility has shown that for stable operation the maximum arc-heater mass flow is about 0.19 kg/sec. At these conditions the heater can deliver 5811 kJ/kg. The total mass flow of the system can be increased from 0.19 kg/sec by adding cold room air downstream of the arc. The final total enthalpy resulting from mixing the two flows will be somewhat less than 5811 kJ/kg, depending on the cold-air mass flow. The interrelation of all these factors can be seen by the following simple development. From figure 1 an energy and mass balance can be written as

$$\dot{m}_1 H_1 + \dot{m}_2 H_2 = \dot{m}_3 H_3 \tag{1}$$

and

$$\dot{m}_1 + \dot{m}_2 = \dot{m}_3 \tag{2}$$

Combining equations (1) and (2) and solving for $\dot{m}_2$ result in

$$\dot{m}_2 = \dot{m}_1 \frac{H_1 - H_3}{H_3 - H_2} \tag{3}$$

The total mass flow is then

$$\dot{m}_3 = \dot{m}_1 \frac{H_1 - H_2}{H_3 - H_2} \tag{4}$$

Now, from continuity,

$$A^* = \frac{\dot{m}_3}{\rho_3{}^* u_3{}^*} = \frac{\dot{m}_1}{\rho_3{}^* u_3{}^*} \frac{H_1 - H_2}{H_3 - H_2}$$

For axisymmetric flow,

$$d^* = \sqrt{\frac{4A^*}{\pi}} = \sqrt{\frac{1.275\dot{m}_1}{\rho_3{}^* u_3{}^*} \frac{H_1 - H_2}{H_3 - H_2}}$$

Let A/A^* be the exit area ratio necessary for the desired exit Mach number at a given enthalpy H_3. Then

$$d = d^*\sqrt{\frac{A}{A^*}} = \sqrt{\frac{1.275\dot{m}_1}{\rho_3{}^* u_3{}^*}\frac{H_1 - H_2}{H_3 - H_2}\frac{A}{A^*}} \tag{5}$$

A plot of equation (5) is shown in figure 2 for an equilibrium gas expanding to $M = 9$. The largest nozzle diameter is obtained with no cold mass flow but at considerable expense to the Reynolds number. Increasing $\dot{m}_2$ increases R_∞ but decreases H_3 and d. On the basis of figure 2 the design point was chosen at $H_3 = 4450$ kJ/kg. This matches the total enthalpy for $M = 9$ flight at an altitude of about 42.7 km. The exit diameter is about 17.8 cm for an equilibrium expansion with a total mass flow of 0.25 kg/sec. If nonequilibrium effects occur, however, the exit diameter will be reduced. To summarize, the selected design stagnation conditions are

$T_t = 3400$ K

$p_t = 100$ atm

$H_t = 4450$ kJ/kg

$\dot{m} = 0.25$ kg/sec

$M_\infty = 9$

At the specified stagnation conditions the composition of air is

$C_{N_2} = 0.7220$

$C_{O_2} = 0.1857$

$C_{NO} = 0.0702$

$C_O = 0.0088$

$C_{Ar} = 0.0129$

The amount of any ionized species is negligible.

Determination of Gas Model

The computer program of Lordi, Mates, and Moselle (ref. 18) for quasi-one-dimensional, nonequilibrium expansion provides a convenient tool for determining the proper gas model for the nozzle-design calculations. The program allows for 11 chemical reactions with species N_2, N, O_2, O, NO, NO^+, Ar, and e^-. Vibration may be either frozen at the stagnation conditions or in equilibrium with the translational and rotational modes. Figure 3 shows the mass-fraction variation of four reacting species along a conical nozzle. Vibration is assumed to be in equilibrium. The mass fractions of the three most abundant species N_2, O_2, and NO freeze very rapidly downstream of the nozzle throat, and thus the composition of the gas is essentially fixed. Figure 4 shows the energy in chemistry for a nonequilibrium expansion. Results are shown for nozzles with two different cone angles (5° and 50°) in order to illustrate the effect of nozzle geometry in the nonequilibrium case. The chemical reactions freeze somewhat sooner in the 50° nozzle than in the 5° nozzle.

Although the chemical reactions freeze early, even in the slower expansion of the 5° cone, the same will not necessarily be true for vibration, since the relaxation rate, in general, is much faster for vibration. The program of reference 18 does not consider vibrational nonequilibrium, and another way of assessing this effect must be found.

An approximate method for treating vibrational nonequilibrium is the sudden-freeze technique of Bray (ref. 19). This useful approximation has found many applications, and it was adapted in reference 20 to the nonequilibrium program of reference 18 by means of the freezing criterion of Phinney (ref. 21). The freeze point for vibration is defined as the point in the expansion where

$$\frac{de_v}{dt} = \frac{e_v}{\tau} \tag{6}$$

In this equation, e_v is the equilibrium vibrational energy of the gas, and τ is the vibrational relaxation time. Usually τ is determined from experimental measurements. Reference 20 used a value for τ obtained from measurements of the vibrational temperature (T_v) of N_2 in air for an expanding flow. For the present paper, use has been made of more recent electron-beam measurements of T_v for N_2 in air (ref. 22). The equation that best fits this data is

$$\tau p = 1.2 \times 10^{-10} \exp\left(\frac{130}{T^{1/3}}\right) \tag{7}$$

In this investigation equation (7) is applied to all three vibrating species, even though O_2, NO, and N_2 do not relax at the same rate. Since the vibrational-temperature measure-

ments are probably accurate to within ±15 percent, at best, and since N_2 does form the bulk of the gas (air), the use of a single vibrational relaxation rate is probably justified. The rates determined in shock-tube studies differ greatly from those determined in nozzle flows (refs. 23 and 24), and it is important that the rate used in this investigation was determined from nozzle measurements. The use of shock-tube values of τ in the program of reference 18 results in vibrational freezing much earlier in the expansion, even upstream of the throat. Figure 5 shows the variation of several τp equations, including the theoretical curve of reference 25 and the experimentally determined curve of reference 26. No attempt has been made here to evaluate the many expressions for τ. Equation (7) which fits the recent data of Sebacher and Guy (ref. 22), is assumed to be adequate.

The freeze criterion of reference 21 was added to the expansion program of reference 18, and the resulting vibrational-energy variation along a conical nozzle is shown in figure 6. The area ratio at which freezing occurs is obviously dependent on nozzle geometry. The chemical reactions in the expansions of figure 6 are assumed to be out of equilibrium, but in fact, the major species freeze quite early in the expansion as was shown in figure 3. Since the energy frozen in chemistry is slightly higher for the 50° expansion (fig. 4), a lower translational temperature occurs downstream; consequently, a lower equilibrium vibration curve is shown in figure 6 for the 50° nozzle.

METHODS AND RESULTS

Method of Characteristics for Equilibrium Flow

Calculating the inviscid contour of a hypersonic nozzle by the method of characteristics (MOC) is a well-known technique that has been in use for many years. With the use of high-speed computers the procedure for equilibrium flow is rapid and straightforward. Nonequilibrium solutions are more difficult to obtain in practice but may be solved by the MOC. The MOC for an equilibrium real gas is discussed in this section, and then a more detailed analysis of the nonequilibrium solution is presented in a subsequent section.

Equilibrium equations.- The equations of motion in natural coordinates for axisymmetric, irrotational, inviscid flow (ref. 27) are

$$\left.\begin{aligned} \frac{M^2 - 1}{U}\frac{\partial U}{\partial s} - \frac{\partial \theta}{\partial n} - \frac{\sin\theta}{r} = 0 \\ \frac{1}{U}\frac{\partial U}{\partial n} - \frac{\partial \theta}{\partial s} = 0 \end{aligned}\right\} \tag{8}$$

From equation (8) the compatibility relations are

$$\frac{dU}{U} \mp \tan \mu \, d\theta - \frac{\sin \theta \sin \mu \tan \mu}{y \cos (\theta \pm \mu)} dx = 0 \tag{9}$$

The characteristic directions are given by

$$\frac{dy}{dx} = \tan(\theta \pm \mu) \tag{10}$$

The characteristic lines are the Mach lines. Figure 7 shows the relationship between the characteristic lines and the streamlines.

Nozzle design by means of the MOC involves writing equations (9) and (10) in difference form and specifying the necessary boundary conditions. Usually the nozzle is divided into several regions, as indicated in figure 8. Region IV is a region of parallel uniform flow at the desired Mach number, region II is a radial-flow region, and regions I and III are transition regions calculated by the MOC. The flow in region II is calculated by means of the radial-flow relation given in reference 3:

$$\left(1 - M^2\right)\frac{dU}{dr} + 2\frac{U}{r} = 0 \tag{11}$$

This may be rewritten as

$$\frac{dr}{r} = \frac{1}{2}\frac{M^2 - 1}{U} dU \tag{12}$$

Equation (12) provides a relation between radial position and velocity and may be integrated directly for a perfect gas. However, for an equilibrium real gas the relation between M and U may not be simply expressed, and a closed-form integration cannot be performed.

The following equation can be obtained from figure 9:

$$\frac{dr}{r} = \frac{d\theta}{\tan \mu} = d\theta\sqrt{M^2 - 1} \tag{13}$$

Combining equations (12) and (13) results in

$$d\theta = \frac{1}{2}\frac{\sqrt{M^2 - 1}}{U} dU \tag{14}$$

This provides a relation between angular position and velocity. Again, for a perfect gas but not for an equilibrium real gas, equation (14) may be integrated immediately. Once a relation between M and U is supplied, the flow properties on the boundaries of the radial-flow region may be determined for a selected exit Mach number. In figure 8, flow properties along the line AB are fixed by selecting a Mach number distribution, and hence a U distribution. The characteristic net in regions I and III can be constructed once the flow properties are determined along segments AB, BC, CD, and DE.

A computer program utilizing a MOC nozzle-calculation procedure similar to that just outlined was developed and reported in reference 9. The relationship between velocity and Mach number for an equilibrium real gas was supplied by tabulated values of $1/M^2$ for various values of $1/U^2$. The Mach number distribution along line AB was assumed to be linear with slope equal to that at the beginning of the radial-flow region. The effects of a real gas on nozzle contours were indicated in reference 9, but the effects of frozen chemistry or frozen vibration in the stagnation chamber are also of interest. Such results should give an idea of the importance of vibrational or chemical nonequilibrium.

The necessary tables of $1/U^2$ as a function of $1/M^2$ for equilibrium or frozen, quasi-one-dimensional flows may be easily computed by means of such computer programs as in reference 18 or reference 28. The program of reference 18 was used to construct four tables assuming (1) chemical equilibrium and vibrational equilibrium, (2) chemical equilibrium and frozen vibration, (3) frozen chemistry and vibrational equilibrium, and (4) frozen chemistry and frozen vibration. Case (2) is unrealistic, since chemistry usually freezes before vibration, but it will serve for comparative purposes. It should be clear that the limiting velocity for frozen flow is reduced by the energy frozen internally, that is, vibrational energy or energy of reaction. The actual limiting velocity is given by

$$u_l^2 = 2(H_t - e_f)$$

The relation between velocity and Mach number must, therefore, vary according to the amount of energy frozen. This shifting effect will assume more importance in the sudden-freeze calculations discussed in the next section.

Figure 10 shows the four nozzle contours calculated by means of the program of reference 9 and the four tables described in the previous paragraph. It is immediately obvious that freezing the vibrational energy has a large effect on the final area ratio needed for Mach 9 flow. The effect seen here is more than simply the removal of a certain amount of energy from that available for the expansion. For vibrational equilibrium the amount of energy in vibration strongly influences the value of γ of the gas and thus appears implicitly in the relation between Mach number and area ratio. Freezing vibration in the

stagnation chamber for the temperature and pressure in figure 10 reduces the exit area ratio by approximately 50 percent for Mach 9 flow. Frozen chemistry reduces the exit area ratio by approximately 20 percent.

Sudden-freeze model.- From the calculations for quasi-one-dimensional flow, it was apparent that the composition of the flow was essentially fixed at its stagnation-chamber value. This left vibration as the only nonequilibrium process. Since the sudden-freeze approximation of a nonequilibrium process had been successfully used in analyses for quasi-one-dimensional flow (refs. 20 and 29), it was adopted in the present MOC calculations. The resulting simplifications are obvious when the compatibility relations for a vibrating diatomic gas are written as

$$\frac{dU}{U} \mp \tan\mu\, d\theta - \frac{\sin\theta \sin\mu \tan\mu}{\cos(\theta \pm \mu)} \frac{dx}{y} = \frac{\sin\mu \tan\mu}{c_{p,a} T_a \cos(\theta \pm \mu)} \frac{\partial e_v}{\partial s} dx$$

$$- \frac{1}{U^2}\left[\frac{T_a dS}{u_\ell^2} + \left(1 - \frac{T_a}{T_v}\right)\frac{de_v}{u_\ell^2}\right] \tag{15}$$

where the subscript a refers to the active degrees of freedom (translation and rotation) and the subscript v refers to vibration. For equilibrium or frozen flow the terms on the right-hand side of equations (15) are zero, and these equations reduce to equations (9). The sudden-freeze model, then, allows the use of the most simple form of the compatibility relations. The characteristic directions for this gas model remain the same as in equations (10). The equilibrium MOC program of reference 9 is easily adapted to this technique by simply calculating the tables of velocity as a function of Mach number for a suddenly frozen gas.

For frozen or equilibrium flow the tables of velocity as a function of Mach number used in the method of reference 9 are independent of geometry, but for the sudden-freeze model these tables are dependent on the freeze point, which, in turn, depends on the geometry. Since the actual geometry is the unknown being sought, an iterative process is necessary. As the first approximation a hyperbolic nozzle contour with 5° asymptote was assumed. The tables thus constructed were used in the MOC calculation to obtain a contour. This proved sufficient for the present case. However, a second iteration may be performed, if desired, by using the calculated contour to generate new tables and, hence, a new contour.

Speed of sound.- It is useful at this point to consider the proper definition of the speed of sound for a nonequilibrium flow. In reference 30, Vincenti and Kruger point out that the speed of sound for equilibrium flow is defined only for an equilibrium state, whereas the

speed of sound for frozen flow is defined for an arbitrary state. For nonequilibrium flow there is no unique speed of propagation that depends only on the conditions in the undisturbed gas. At the frozen and equilibrium limits the small-disturbance equation exhibits a singular drop in order, but arbitrarily close to equilibrium the frozen speed of sound retains its meaning, whereas the equilibrium speed of sound does not. Sedney et al. (ref. 31) and references 32, 33, and 34 have concluded that the frozen speed of sound is the correct value on which to base the characteristics, even very close to equilibrium.

In the present case the sudden-freeze concept results in a discontinuous change in Mach number from the equilibrium value to the frozen value at the freeze point. In order to avoid this discontinuity, the frozen speed of sound was used even in the equilibrium region for the present MOC calculations. This seems to be consistent with the discussion in references 30 and 31.

Tables of velocity as a function of Mach number.- The necessary table for use in the program of reference 9 may be constructed for the sudden-freeze model by using the following development. The energy equation is

$$H_t = h + \frac{u^2}{2} \tag{16}$$

The limiting velocity is defined by

$$u_l = \sqrt{2H_t}$$

and

$$U = \frac{u}{u_l}$$

Equation (16) becomes

$$\frac{1}{U^2} = \frac{H_t}{H_t - h} \tag{17}$$

Now,

$$h = c_{p,a}T_a + e_v$$

and

$$M_a^2 = \frac{u^2}{a^2} = \frac{u^2}{\gamma_a R_s T_a}$$

Therefore,

$$h = c_{p,a} \frac{u^2}{M_a^2} \frac{1}{\gamma_a R_s} + e_v \tag{18}$$

After some algebraic manipulations, equation (17), with the use of equation (18), becomes

$$\frac{1}{U^2}\left(1 - \frac{e_v}{H_t}\right) = 1 + \frac{2}{\gamma_a - 1} \frac{1}{M_a^2} \tag{19}$$

which expresses the desired relationship between frozen Mach number and velocity. For a nonvibrating gas, equation (19) reduces to the familiar perfect-gas relation. The term on the right-hand side of equation (19) passes smoothly through the freeze point, since it contains the frozen Mach number M_a. The $1/U^2$ term, however, poses some difficulty because the limiting velocity is defined in terms of the total energy available for the expansion. At the freeze point, a certain amount of energy is "locked" in vibration and becomes unavailable for conversion to velocity. Thus the limiting velocity before freezing is

$$u_l = \sqrt{2H_t} \tag{20}$$

and after freezing is

$$u_l = \sqrt{2\left(H_t - e_f\right)} \tag{21}$$

Of course, if chemistry is frozen in the stagnation chamber, as has been assumed here, then the total stagnation enthalpy H_t is reduced by that amount initially.

Figure 11(a) shows the variation of $1/U^2$ with $1/M_a^2$ for a hyperbolic expansion with chemistry frozen in the stagnation chamber and vibration frozen downstream of the throat. Curves are shown for the two different expressions for u_l (eqs. (20) and (21)). Figure 11(b) shows the freeze-point region to a larger scale. The smooth curve through the discontinuity is strictly an arbitrarily faired transition curve. The possibilities for constructing the tables of velocity as a function of Mach number are

(1) Use equation (20) for the complete expansion
(2) Use equation (21) for the complete expansion

(3) Use an arbitrary transition between equations (20) and (21) in the freeze-point region.

Without some rational basis for choosing the transition curve the use of method (3) seems unrealistic, since the choice of the transition curve amounts to assuming a vibration relaxation rate. The easiest choice would be to use the equilibrium definition (eq. (20)) for the complete expansion, since the freeze point occurs at small values of e_v. Actually, nozzle designs computed by methods (1), (2), and (3) in the construction of these tables showed negligible differences in contour, as can be seen in figure 12. This is not surprising in view of the small amount of energy frozen in vibration. For example, at $1/U^2 = 4.0$ (fig. 11(a)) the change in M_a between the two curves is only about 3 percent. At higher Mach numbers the percentage change is even less.

Figure 13 shows the complete contour generated from the program of reference 9 for a sudden-freeze gas model. As expected, the exit area ratio for this nozzle falls between that for the vibrational-equilibrium nozzle and that for the frozen-vibration nozzle, and the exit diameter of this nozzle meets the size requirements mentioned previously. The design conditions fix the throat radius at 0.350 cm, and therefore the exit diameter is 15.20 cm. Thus, vibrational freezing reduced the exit diameter by more than 14 percent from the original value for an equilibrium expansion (17.8 cm). Although the nozzle contour is smooth and the exit diameter is of the right order, there is no assurance that this approximate design will provide a Mach 9 uniform flow when vibrational-nonequilibrium effects are present. That is, the nonequilibrium effects on nozzle contour are only approximated by the sudden-freeze model, and consequently the contour may be wrong. In order to assess the usefulness of the sudden-freeze design, a detailed analysis of the effects of vibrational nonequilibrium on flow through a given nozzle was undertaken. The results of this analysis are given in the next section.

Method of Characteristics for Nonequilibrium Flow

The MOC for nonequilibrium nozzle flows has been treated by a number of authors (refs. 13 to 15 and 35 to 37, e.g.). Sedney (ref. 15) surveyed many of these methods and concluded that although much effort has been expended, there are still many uncertainties as to the particular grid scheme and starting procedures that should be used. Sedney also points out that most methods deal with what is called the direct problem, that is, determining the flow in a nozzle of given contour. This is unsuitable for calculation of the nozzle contour necessary to produce a specific final test-section flow (the indirect problem). However, the sudden-freeze nozzle design generated in the previous section can be analyzed by means of one of these direct methods. One such direct analysis is the method of reference 38. This method was written for internal flows with mixing and combustion, but it was modified for the present problem to treat an inviscid flow with vibrational nonequilibrium. In order to show clearly the vibrational terms in the compatibility relations for

a reacting, inviscid, vibrating gas, these relations are shown in a form different from equations (15) but in a form similar to that presented in reference 38.

Equations of motion.- The equations of motion are

Energy

$$c_{p,a}\rho u \frac{\partial T_a}{\partial s} + \rho u^2 \frac{\partial u}{\partial s} = -\rho u \sum_i C_i \frac{\partial e_{v,i}}{\partial s} - \sum_i h_i \dot{w}_i \tag{22}$$

where

$$c_{p,a} = \sum_i C_i c_{p,a,i}$$

The additional term due to vibration is immediately evident. The other equations are

Continuity

$$\frac{1}{\rho}\frac{\partial \rho}{\partial s} + \frac{1}{u}\frac{\partial u}{\partial s} + \frac{\partial \theta}{\partial n} + \frac{\sin \theta}{y} = 0 \tag{23}$$

n-momentum

$$\rho u^2 \frac{\partial \theta}{\partial s} = -\frac{\partial p}{\partial n} \tag{24}$$

s-momentum

$$\rho u \frac{\partial u}{\partial s} = -\frac{\partial p}{\partial s} \tag{25}$$

State

$$p = \rho T_a R\left(\sum_i \frac{C_i}{W_i}\right) \tag{26}$$

Relaxation rate

$$\frac{\partial e_{v,i}}{\partial s} = \frac{e_{v,i}(T_a) - e_{v,i}(T_v)}{\tau u} \tag{27}$$

Compatibility relations.- The compatibility relations may be derived from equations (22) to (27). Reference 39 gives a detailed derivation resulting in the following nondimensional equations:

$$\frac{\sin \mu_a \cos \mu_a}{\gamma_a \bar{p}} d\bar{p} \pm d\theta + \left[\frac{\sin \theta}{\bar{y}} + \frac{1}{\bar{c}_{p,a} \bar{T}_a} \sum_i C_i \frac{\partial \bar{e}_{v,i}}{\partial \bar{s}} + \frac{\gamma_a - 1}{\gamma_a (\gamma_\infty - 1)} \frac{\sum_i \bar{h}_i \dot{\bar{w}}_i}{M_\infty^2 \bar{p} \bar{u}} - \frac{\gamma_a - 1}{\gamma_a (\gamma_\infty - 1)} \frac{W \sum_i \frac{\dot{\bar{w}}_i}{\bar{W}_i}}{M_\infty^2 \bar{p} \bar{u}} \right] \frac{\sin \mu_a}{\cos(\theta \pm \mu_a)} d\bar{x} = 0 \quad (28)$$

Equations (28) are similar to the compatibility relations given by Dash in reference 38 except for the appearance of the vibrational-energy term.

Design analysis.- Equations (28) were used to modify the program of reference 38 for the case of chemically frozen air with vibrational nonequilibrium. Reference 39 describes the changes made and gives a complete listing of the modified program. Essentially, the chemistry package in reference 38 was replaced by the vibrational terms for N_2, O_2, and NO, so that, unlike the original program, no chemistry option was available. All species containing hydrogen and all diffusive terms were deleted.

The resulting program was used to analyze the flow in the sudden-freeze nozzle design of figure 13. The computed exit profiles are shown in figure 14. The largest nonuniformity across the exit appeared in the pressure, which increased by about 10 percent from the center line to the inviscid-core edge. The temperature increased approximately 3 percent away from the center line, while the velocity varied less than 0.2 percent. The Mach number was relatively uniform across the nozzle exit but was approximately 3 percent below the design value of 9. The dynamic-pressure variation was about 7 percent, and the flow angularity was negligible (less than 0.1°). For many applications the nonuniformities present in this nozzle are acceptable, especially considering the approximate nature of its design. The vibrational-energy distribution along the nozzle center line is shown in figure 15. The nearly constant value of energy above $\frac{x}{r^*} = 40$ indicates frozen vibration.

Off-design analysis.- In arc-tunnel testing it is important that small variations in stagnation conditions do not significantly disturb the quality of the test-section flow, since, in many instances, exact duplication of stagnation conditions from run to run is impossible. A limited analysis of off-design stagnation conditions for the sudden-freeze nozzle of figure 13 was conducted. Figure 16(a) shows the effect on the exit profiles of a 10-percent decrease in stagnation pressure, and figure 16(b) shows the effect of a 10-percent increase

in stagnation temperature. In figure 16(c) both pressure and temperature have been reduced by 10 percent. In all three cases flow uniformity is similar to the design case. Figure 16(d) shows exit profiles for a 35-percent-lower stagnation pressure and a 25-percent-lower stagnation temperature. The maximum flow angularity has increased almost 20 percent over its maximum at the design conditions. Thus, large deviations from the design conditions may be harmful to the flow quality, since actual nonequilibrium processes are strongly dependent on stagnation conditions.

CONCLUDING REMARKS

The present investigation has treated the approximate design of a nozzle with nonequilibrium flow. Calculations for quasi-one-dimensional flow indicated that for conical expansions of 5° and 50° at the desired stagnation conditions of 100 atm and 3400 K, chemical reactions were essentially frozen in the stagnation chamber and vibration was the only nonequilibrium process. The nonequilibrium vibration was approximated by the sudden-freeze concept in which the three vibrating species, N_2, O_2, and NO, were all assumed to freeze simultaneously. An empirically determined relaxation rate for N_2 in expanding air was used to determine the freeze point. An existing equilibrium characteristics program was modified to produce a nozzle contour with vibrational sudden freezing. Since freezing occurred for the present conditions at low values of vibrational energy, this contour was found to be insensitive to shifts in the relationship between velocity and Mach number caused by freezing the vibrational mode. This simplified the calculations through the freeze-point region by allowing use of a single expression for the limiting velocity.

The approximate contour thus generated was analyzed for design conditions by modifying an existing direct characteristics program to account for vibrational nonequilibrium. The exit Mach number was approximately 3 percent lower than the design value of 9 but was still very uniform across the nozzle exit. The temperature and velocity profiles indicated only minor variations (less than 0.2 percent in velocity and less than 3 percent in temperature), but the pressure varied by as much as 10 percent from the center line to the core edge. The dynamic-pressure variation was slightly less than 7 percent. Overall, however, the inviscid contour generated by this approximate method gave exit profiles considered acceptable for the present application.

Analysis of the operation of this nozzle at slightly off-design stagnation conditions (± 10 percent in pressure and temperature) indicated no appreciable additional exit nonuniformities. However, at a pressure 35 percent below and a temperature 25 percent below the design values, the maximum flow angularity was increased almost 20 percent over the design value. This, of course, indicates that at stagnation conditions far removed from the design values, the nonequilibrium effects are no longer properly accounted for in the contour and may cause a nonuniform exit flow.

This study indicates that an approximate treatment of a single nonequilibrium process (vibration) can be used to compute the inviscid contour of a hypersonic, axisymmetric nozzle with vibrational nonequilibrium and that the contour thus generated exhibits reasonably uniform exit profiles. The advantage of this approximate method lies in the fact that the designer may use existing computer programs and therefore save considerable time and effort.

Langley Research Center,
National Aeronautics and Space Administration,
Hampton, Va., November 25, 1974.

REFERENCES

1. Foelsch, Kuno: The Analytical Design of an Axially Symmetric Laval Nozzle for a Parallel and Uniform Jet. J. Aeronaut. Sci., vol. 16, no. 3, Mar. 1949, pp. 161-166, 188.

2. Cresci, Robert J.: Tabulation of Coordinates for Hypersonic Axisymmetric Nozzles. WADD Tech. Note 58-300, Pts. I and II, U.S. Air Force.
   Part I – Analysis and Coordinates for Test Section Mach Numbers of 8, 12 and 20, DDC Doc. No. AD 204 213, Oct. 1958.
   Part II – Coordinates for Test Section Mach Numbers of 6, 7, 8.5, 9, 10, 14, 16, and 18, DDC Doc. No. AD 240 666, July 1960.

3. Beckwith, Ivan E.; Ridyard, Herbert W.; and Cromer, Nancy: The Aerodynamic Design of High Mach Number Nozzles Utilizing Axisymmetric Flow With Application to a Nozzle of Square Test Section. NACA TN 2711, 1952.

4. Sauerwein, Harry: A General Numerical Method of Characteristics. AIAA Paper No. 65-25, Jan. 1965.

5. Edenfield, E. E.: Contoured Nozzle Design and Evaluation for Hotshot Wind Tunnels. AIAA Paper No. 68-369, Apr. 1968.

6. Moger, W. C.; and Ramsay, D. B.: Supersonic Axisymmetric Nozzle Design by Mass Flow Techniques Utilizing a Digital Computer. AEDC-TDR-64-110, U.S. Air Force, June 1964. (Available from DDC as AD 601 589.)

7. Potter, J. L.; and Carden, W. H.: Design of Axisymmetric Contoured Nozzles for Laminar Hypersonic Flow. AIAA Paper No. 68-372, Apr. 1968.

8. Sivells, James C.: Aerodynamic Design of Axisymmetric Hypersonic Wind Tunnel Nozzles. AIAA Paper No. 69-337, Apr. 1969.

9. Johnson, Charles B.; Boney, Lillian R.; Ellison, James C.; and Erickson, Wayne D.: Real-Gas Effects on Hypersonic Nozzle Contours With a Method of Calculation. NASA TN D-1622, 1963.

10. Guentert, Eleanor Costilow; and Neumann, Harvey E.: Design of Axisymmetric Exhaust Nozzles by Method of Characteristics Incorporating a Variable Isentropic Exponent. NASA TR R-33, 1959.

11. Ehlers, Edward F.: The Method of Characteristics for the Supersonic Flow of an Ideal Dissociating Gas. I. Equilibrium Flow. Math. Note No. 355 (D-82-0364), Math. Res. Lab., Boeing Sci. Res. Lab., July 1964.

12. Glowacki, Walter J.: FORTRAN IV (IBM 7090) Program for the Design of Contoured Axisymmetric Nozzles for High Temperature Air. NOLTR 64-219, U.S. Navy, Feb. 10, 1965. (Available from DDC as AD 465 605.)

13. Enkenhus, K. R.: Axisymmetric Nozzle Flows Including Non-Equilibrium Effects. Theoretical Inviscid Fluid Mechanics, R. E. Wilson, compiler, NOLTR 66-191, U.S. Navy, Sept. 26, 1966, pp. 3-1 – 3-32. (Available from DDC as AD 642 771.)

14. Walitt, Leonard; and Nagai, D. T.: Theoretical and Experimental Studies of Two-Dimensional Chemical Nonequilibrium Flow in Exhaust Expansion Systems. Rep. No. 25,067 (Contract AF 33(657)-8419), Marquardt Corp., Jan. 15, 1963.

15. Sedney, Raymond: Some Aspects of Non-Equilibrium Flows. Rep. No. 1099, Ballistic Res. Lab., Aberdeen Proving Ground, Mar. 1960.

16. Sedney, Raymond: A Survey of the Method of Characteristics for Nonequilibrium, Internal Flows. AIAA Paper No. 69-6, Jan. 1969.

17. Boatright, W. B.; Sebacher, D. I.; Guy, R. W.; and Duckett, R. J.: Review of Testing Techniques and Flow Calibration Results for Hypersonic Arc Tunnels. AIAA Paper No. 68-379, Apr. 1968.

18. Lordi, J. A.; Mates, R. E.; and Moselle, J. R.: Computer Program for the Numerical Solution of Nonequilibrium Expansions of Reacting Gas Mixtures. NASA CR-472, 1966.

19. Bray, K. N. C.: Atomic Recombination in a Hypersonic Wind-Tunnel Nozzle. J. Fluid Mech., vol. 6, pt. 1, July 1959, pp. 1-32.

20. Guy, Robert W.: A Calibration and Diagnosis of the Test Stream of an Electric Arc-Heated Wind Tunnel. M.A.E. Thesis, Univ. of Virginia, Sept. 1969.

21. Phinney, R.: Criterion for Vibrational Freezing in a Nozzle Expansion. AIAA J., vol. 1, no. 2, Feb. 1963, pp. 496-497.

22. Sebacher, Daniel I.; and Guy, Robert W.: Vibrational Relaxation in Expanding N_2 and Air. NASA TM X-71988, 1974.

23. Hurle, I. R.; Russo, A. L.; and Hall, J. Gordon: Experimental Studies of Vibrational and Dissociative Nonequilibrium in Expanded Gas Flows. [Preprint] 63-439, Amer. Inst. Aeronaut. Astronaut., Aug. 1963.

24. MacDermott, W. N.; and Marshall, J. C.: Theoretical and Experimental Nonequilibrium Expansions of Partially-Dissociated Air. AIAA Paper No. 69-328, Apr. 1969.

25. Schwartz, R. N.; Slawsky, Z. I.; and Herzfeld, K. F.: Calculation of Vibrational Relaxation Times in Gases. J. Chem. Phys., vol. 20, no. 10, Oct. 1952, pp. 1591-1599.

26. White, Donald R.; and Millikan, Roger C.: Vibrational Relaxation in Air. AIAA J., vol. 2, no. 10, Oct. 1964, pp. 1844-1846.

27. Liepmann, H. W.; and Roshko, A.: Elements of Gasdynamics. John Wiley & Sons, Inc., c.1957.

28. Emanuel, George; and Vincenti, Walter G.: Method for Calculation of the One-Dimensional Nonequilibrium Flow of a General Gas Mixture Through a Hypersonic Nozzle. AEDC-TDR-62-131, U.S. Air Force, June 1962. (Available from DDC as AD 276 822.)

29. Tirumalesa, Duvvuri: Nozzle Flows With Coupled Vibrational and Dissociational Non-equilibrium. AIAA Paper No. 66-520, June 1966.

30. Vincenti, Walter G.; and Kruger, Charles H., Jr.: Introduction to Physical Gas Dynamics. John Wiley & Sons, Inc., c.1965.

31. Sedney, R.; South, J. C.; and Gerber, N.: Characteristic Calculation of Non-Equilibrium Flows. Rep. No. 1173, Ballistic Res. Labs., Aberdeen Proving Ground, Apr. 1962.

32. Chu, Boa-Teh: Wave Propagation and the Method of Characteristics in Reacting Gas Mixtures With Applications to Hypersonic Flow. WADC TN 57-213, DDC Doc. No. AD 118 350, U.S. Air Force, May 1957.

33. Moore, Franklin K.; and Gibson, Walter E.: Propagation of Weak Disturbances in a Gas Subject to Relaxation Effects. J. Aero/Space Sci., vol. 27, no. 2, Feb. 1960, pp. 117-127.

34. Wood, William W.; and Parker, F. R.: Structure of a Centered Rarefaction Wave in a Relaxing Gas. Phys. Fluids, vol. 1, no. 3, May-June 1958, pp. 230-241.

35. Zupnik, T. F.; Nilson, E. N.; Landis, F.; Keilbach, J. R.; and Ables, D.: Application of the Method of Characteristics Including Reaction Kinetics to Nozzle Flow. AIAA Preprint No. 64-97, Jan. 1964.

36. Widawsky, A.: Computer Program for the Determination of Chemically Reacting Flow Fields by the Method of Characteristics. RTD-TDR-63-4286, U.S. Air Force, Oct. 31, 1963. (Available from DDC as AD 437 698.)

37. Der, James J.: Theoretical Studies of Supersonic Two-Dimensional and Axisymmetric Nonequilibrium Flow, Including Calculations of Flow Through a Nozzle. NASA TR R-164, 1963.

38. Dash, S.: An Analysis of Internal Supersonic Flows With Diffusion, Dissipation and Hydrogen-Air Combustion. NACA CR-111783, 1970.

39. Anders, John B., Jr.: The Design of a Hypersonic, Arc-Jet Nozzle With Vibrational Nonequilibrium. M.S. Thesis, George Washington Univ., 1972.

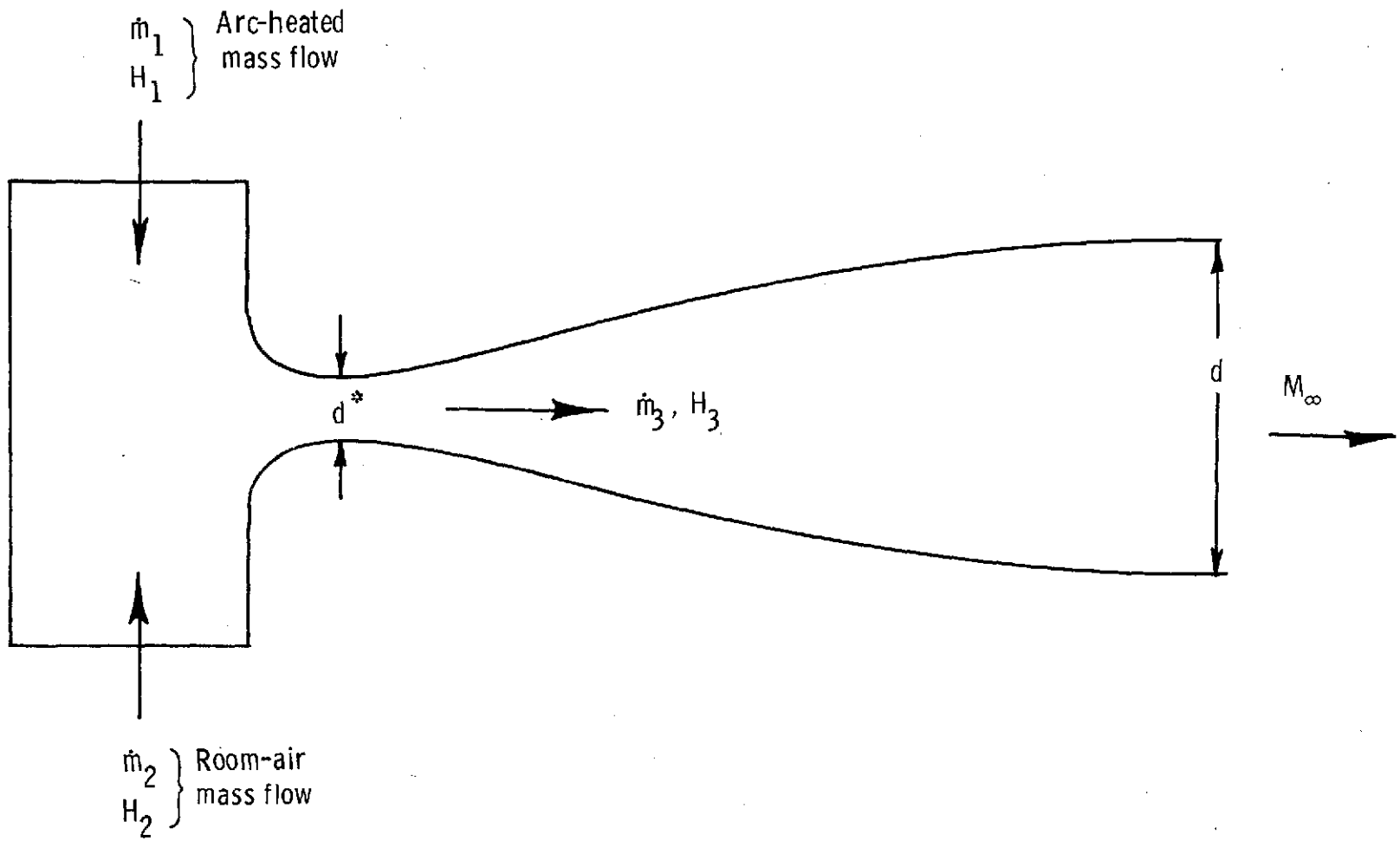

Figure 1.- Schematic of energy and mass-flow balance.

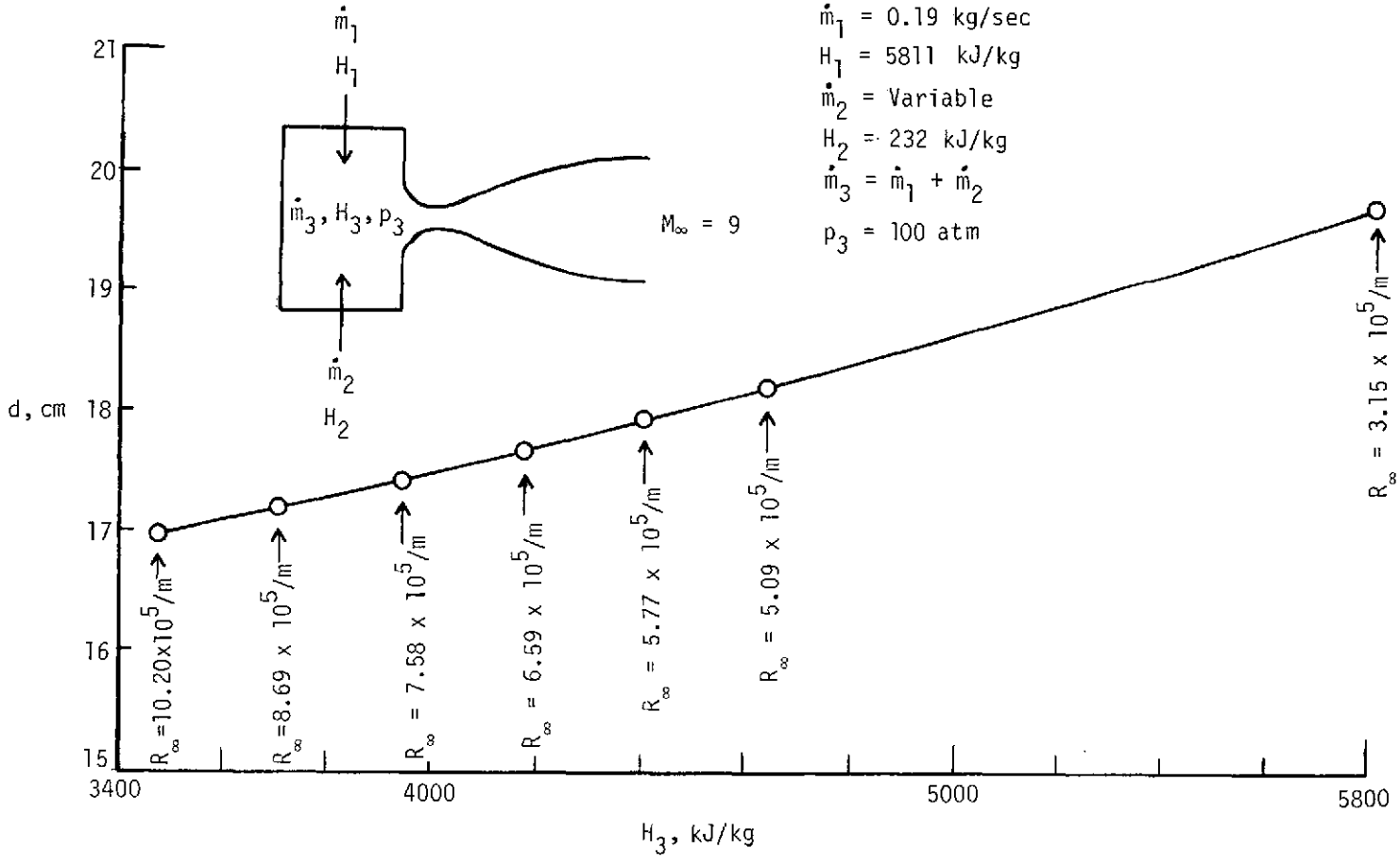

Figure 2.- Variation of exit diameter with stagnation enthalpy.

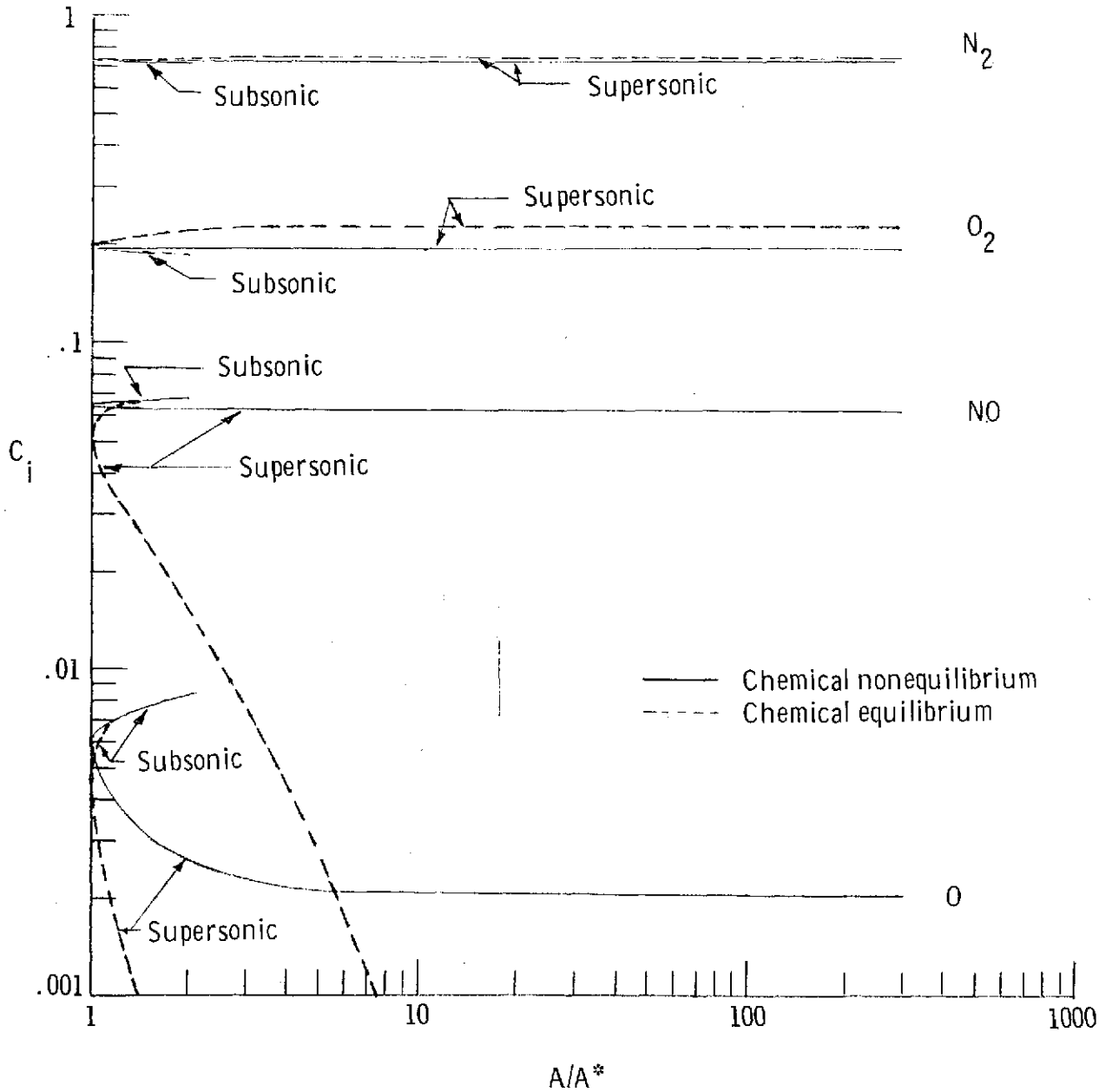

Figure 3.- Mass fractions of reacting species with vibrational equilibrium in a 5° conical nozzle. p_t = 100 atm; T_t = 3400 K.

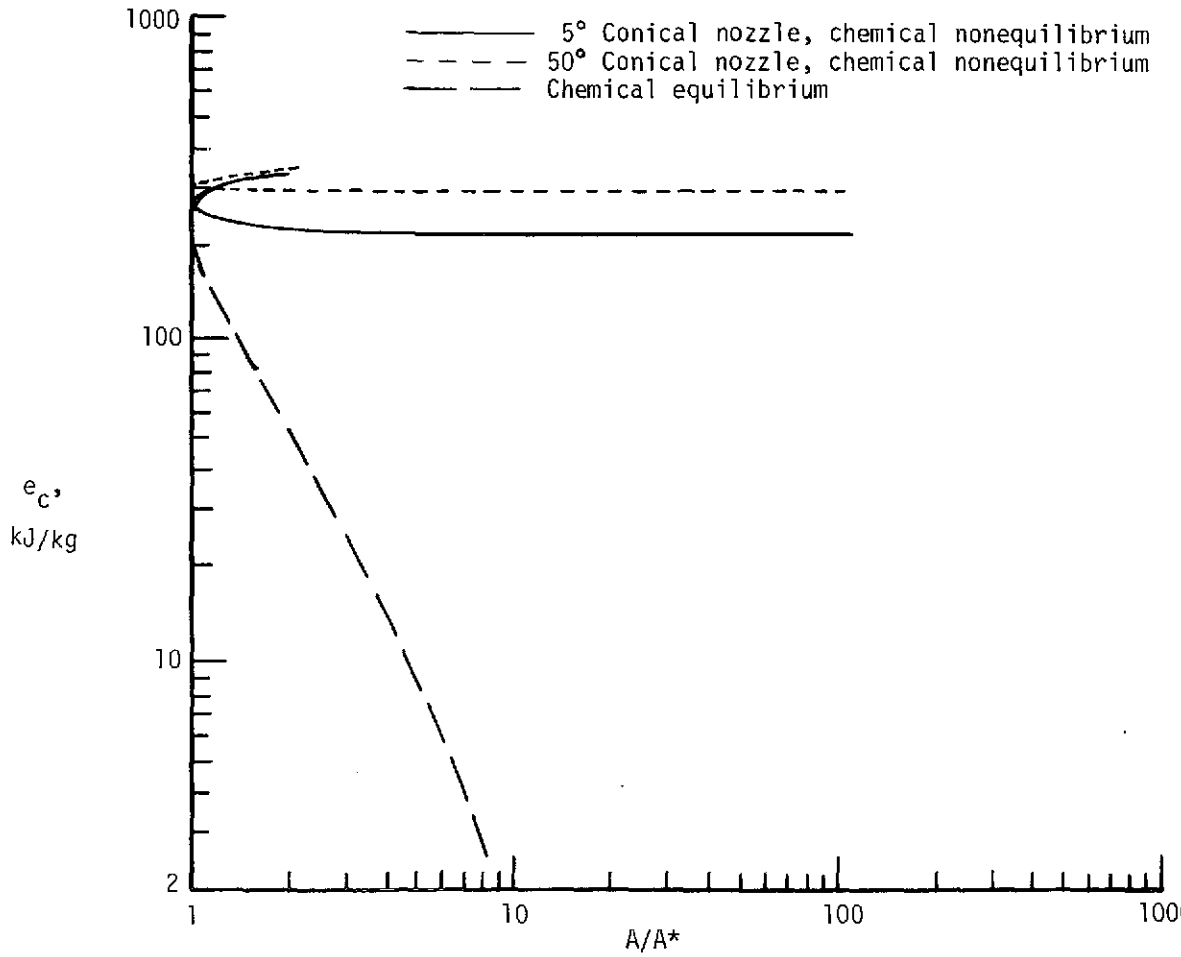

Figure 4.- Energy in formation of chemical species for conical expansions. Vibrational equilibrium; p_t = 100 atm; T_t = 3400 K.

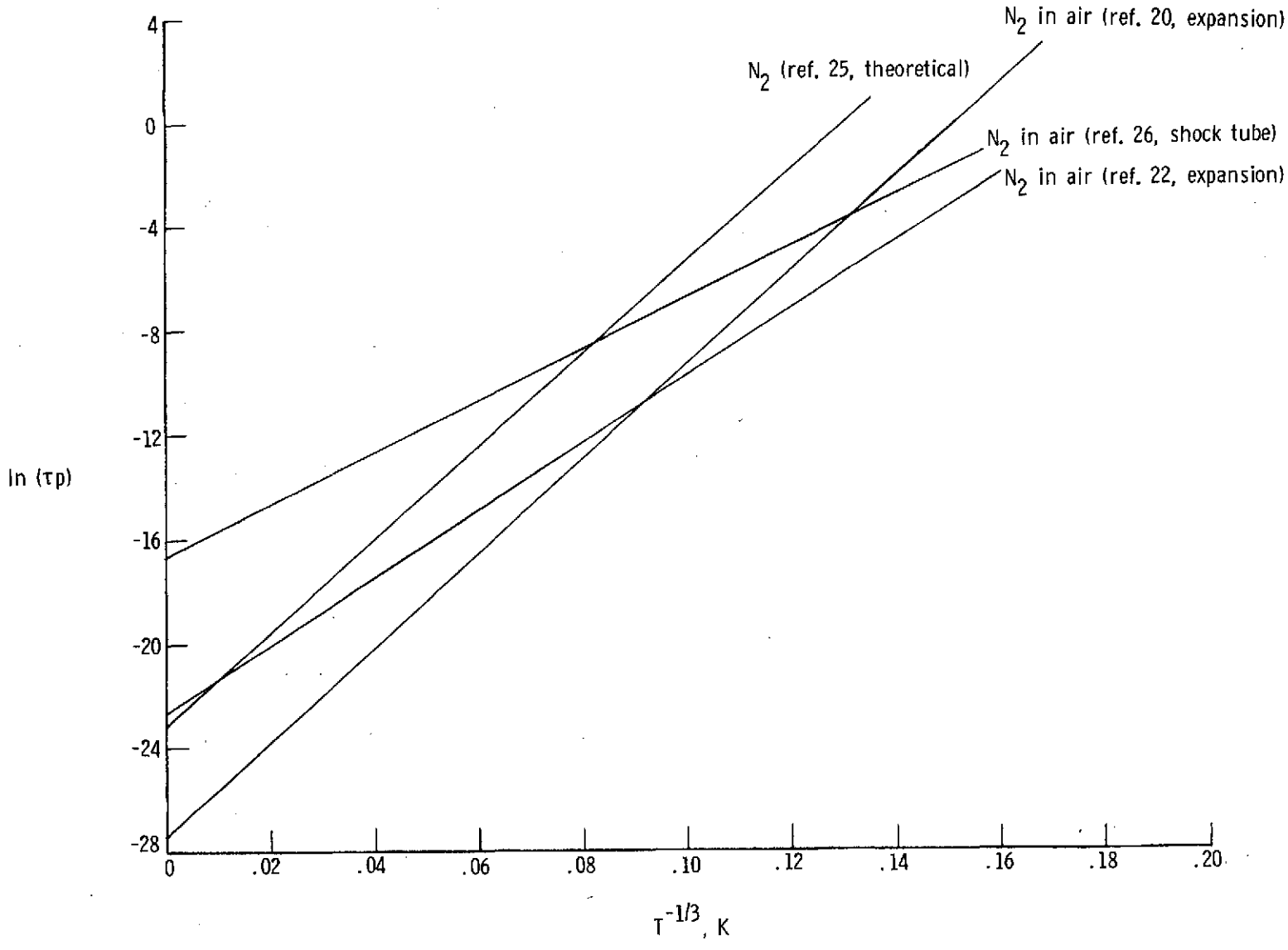

Figure 5.- Variation of vibrational relaxation rate with temperature. (τp is in atm-sec.)

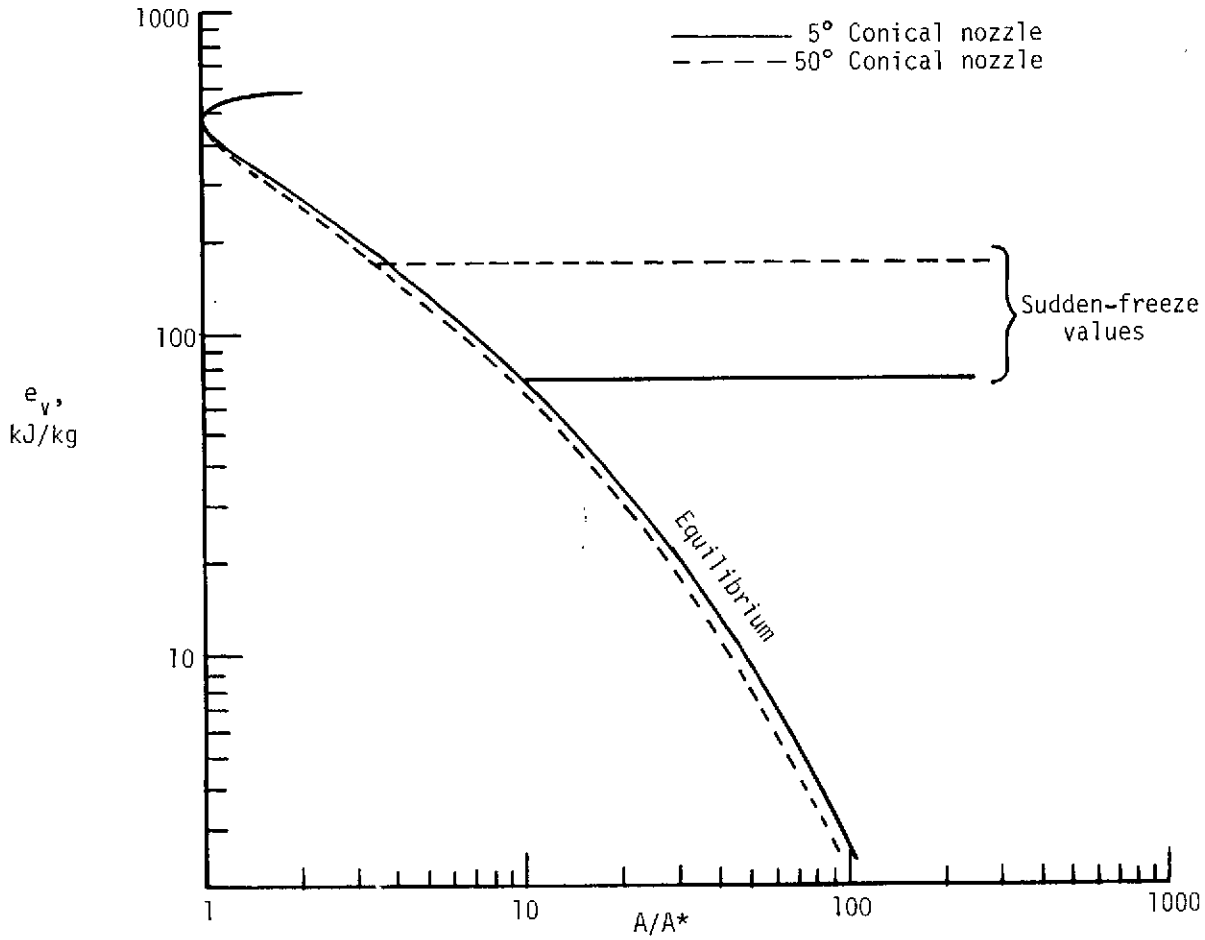

Figure 6.- Energy in vibration for conical expansions. Chemical nonequilibrium; p_t = 100 atm; T_t = 3400 K.

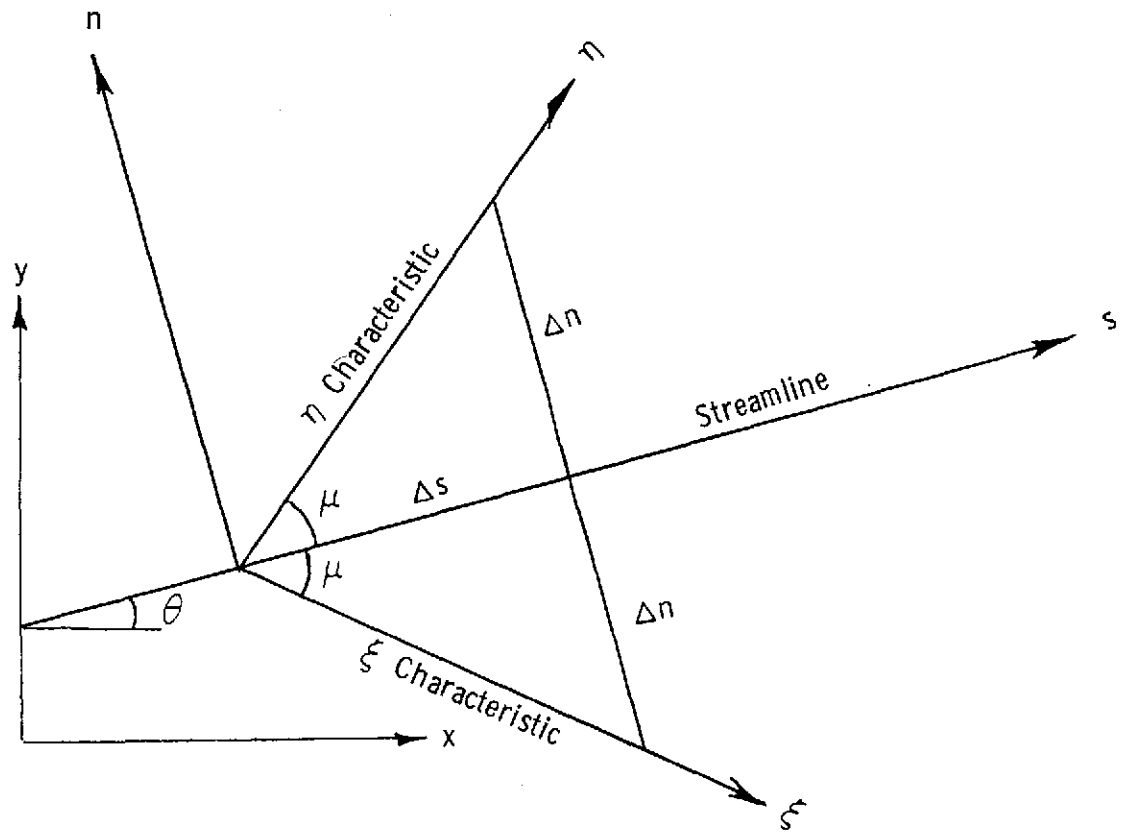

Figure 7.- Relation between characteristic directions and nozzle coordinate system.

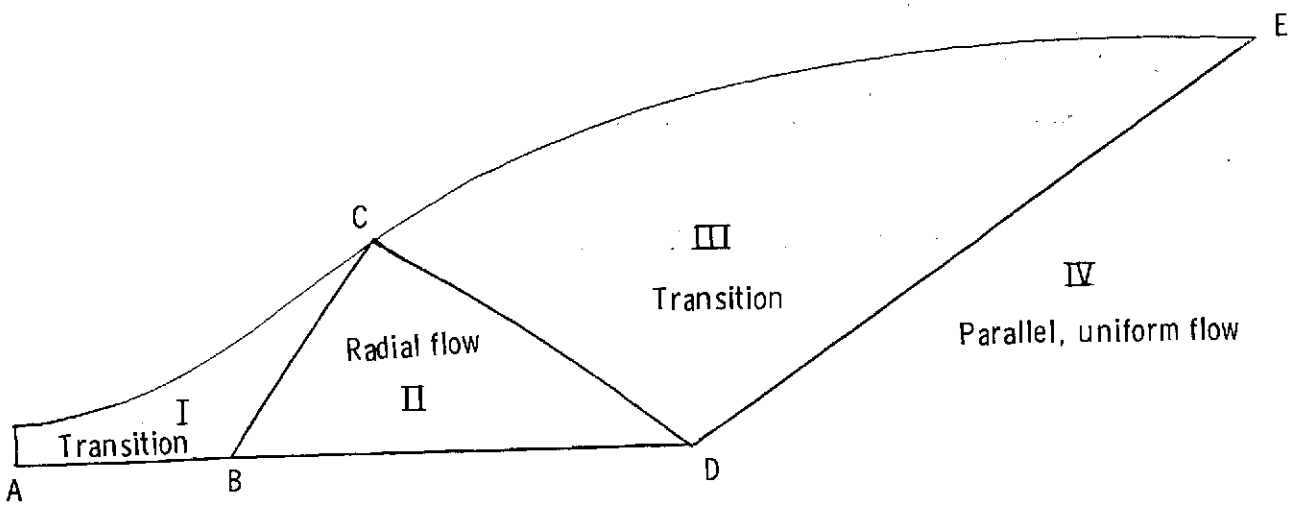

Figure 8.- Nozzle divisions for MOC calculation.

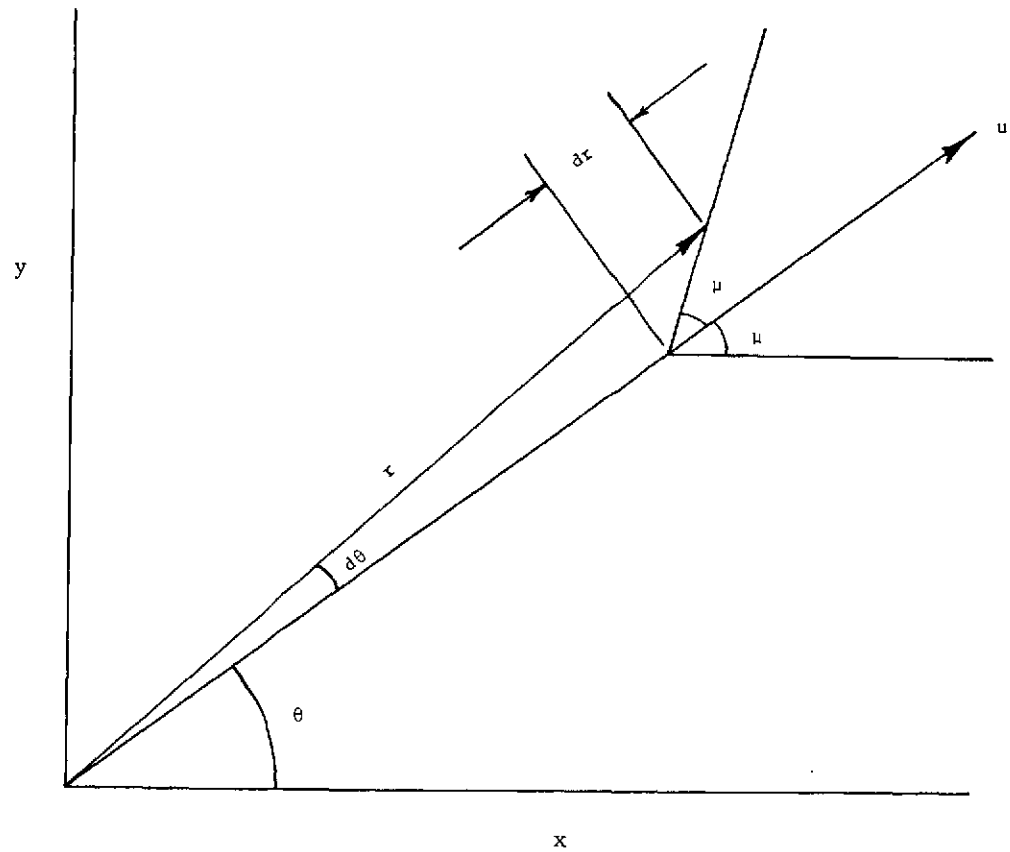

Figure 9.- Radial-flow coordinate system.

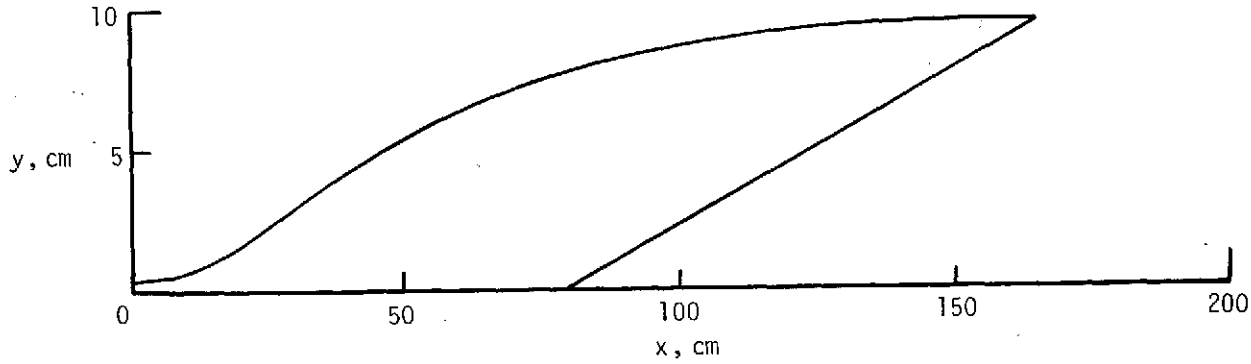

(a) Chemical equilibrium, vibrational equilibrium.

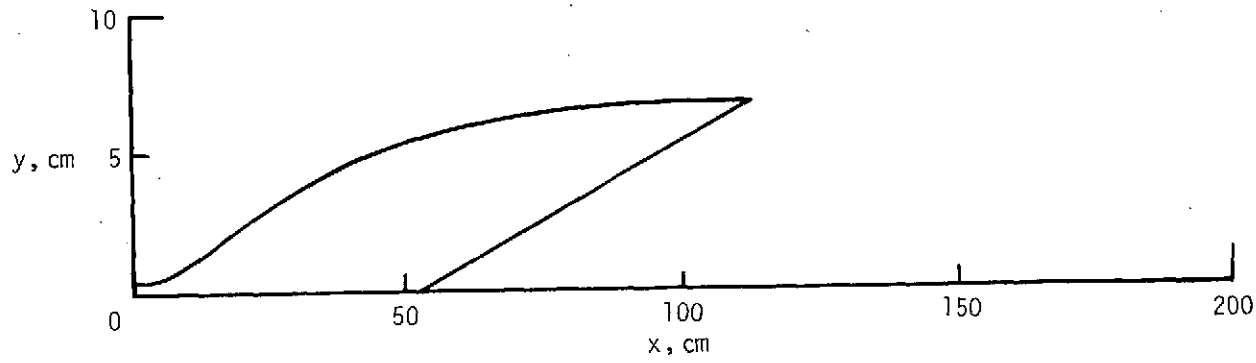

(b) Chemical equilibrium, frozen vibration.

Figure 10.- Nozzle contours for equilibrium and frozen flows.
p_t = 100 atm; T_t = 3400 K; M_∞ = 9.

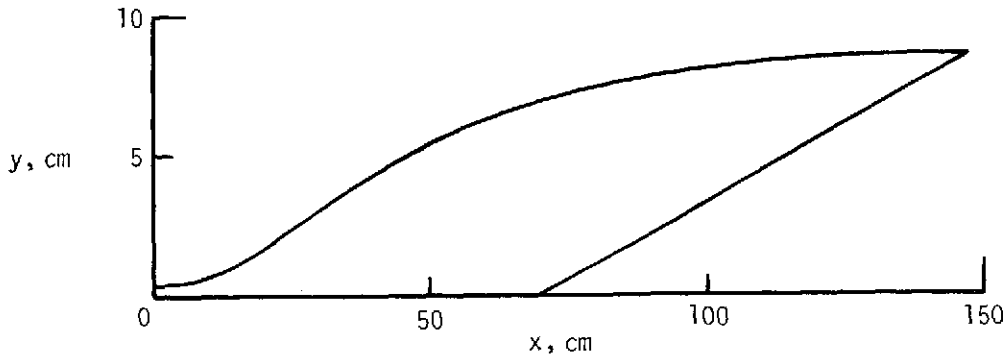

(c) Frozen chemistry, vibrational equilibrium.

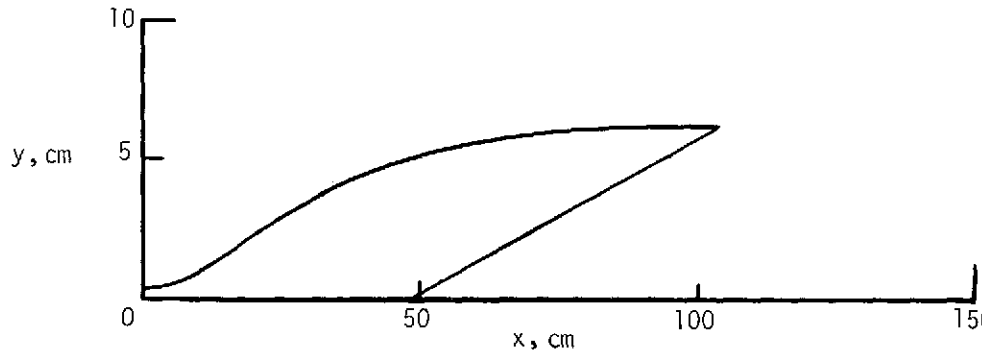

(d) Frozen chemistry, frozen vibration.

Figure 10.- Concluded.

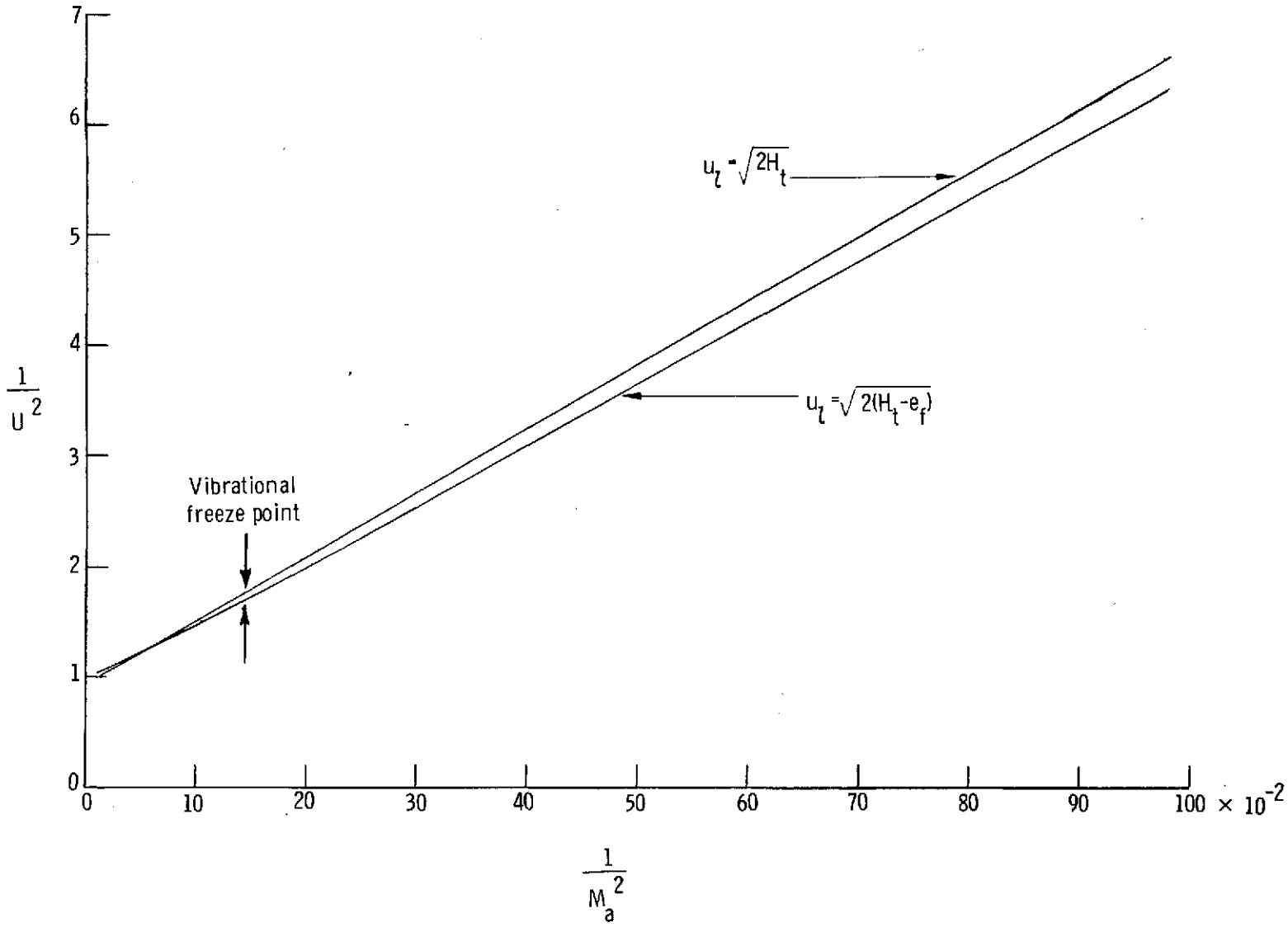

(a) Large-scale variation.

Figure 11.- Velocity-ratio variation with frozen Mach number. p_t = 100 atm; T_t = 3400 K.

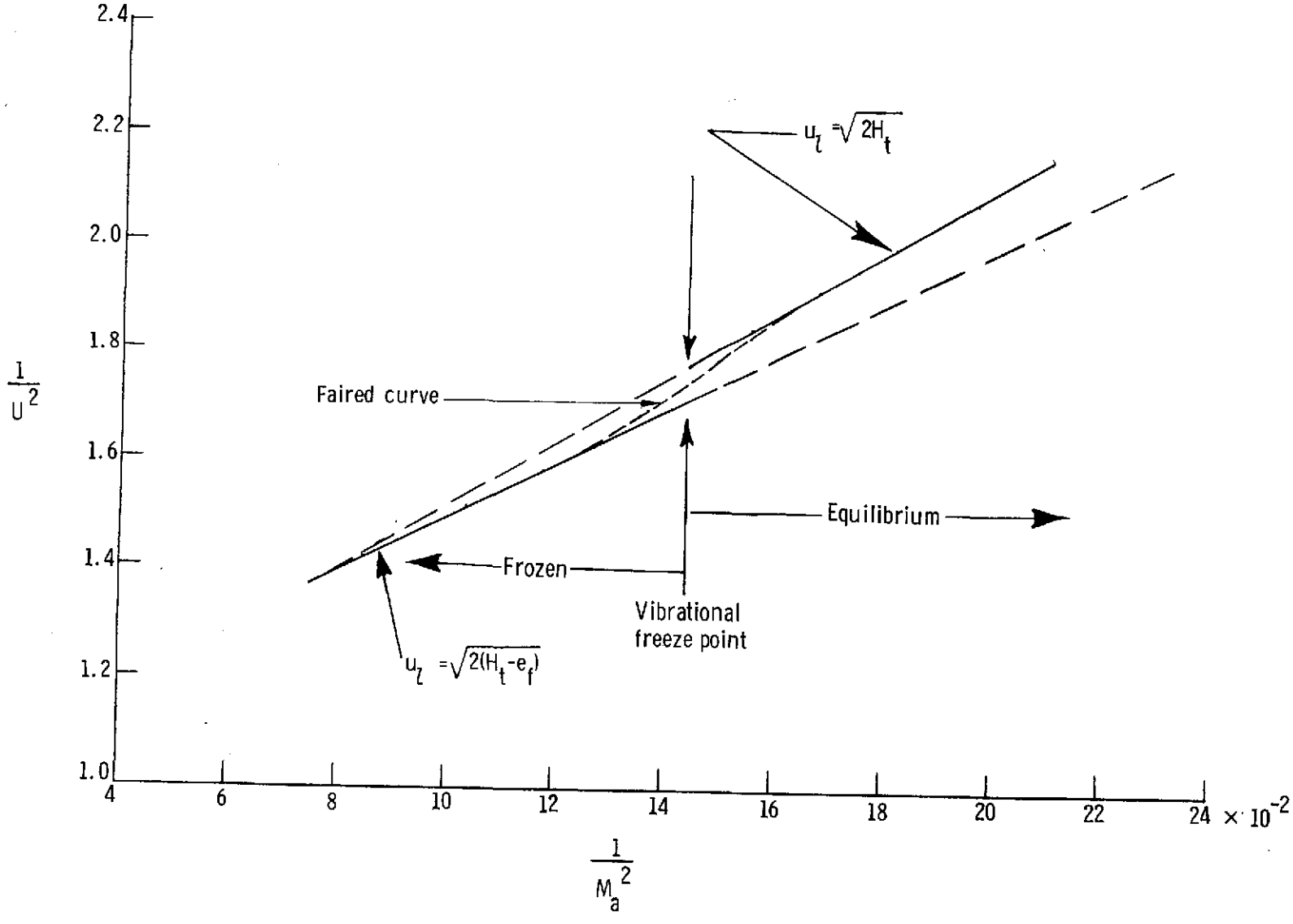

(b) Freeze-point region.

Figure 11.- Concluded.

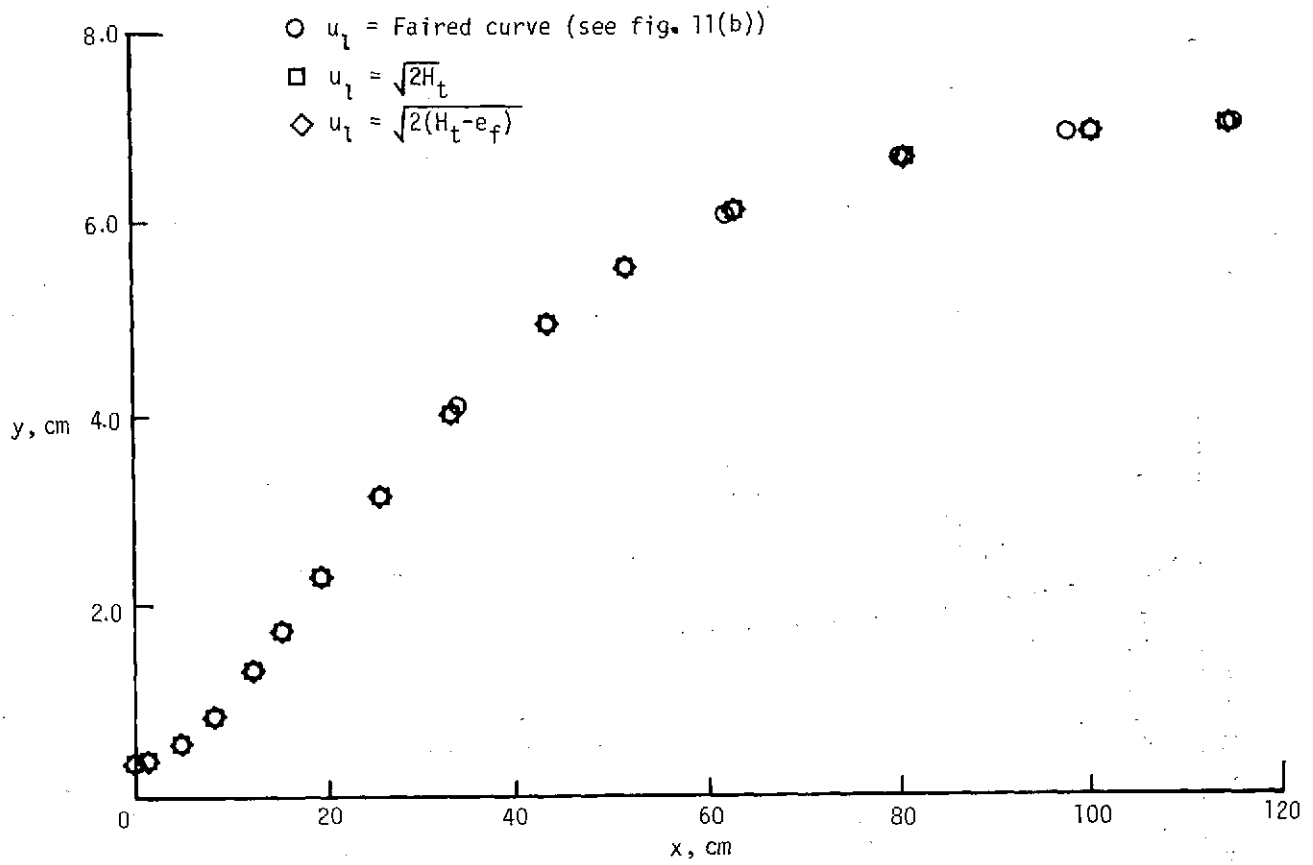

Figure 12.- Variation of nozzle contour with limiting-velocity definition.

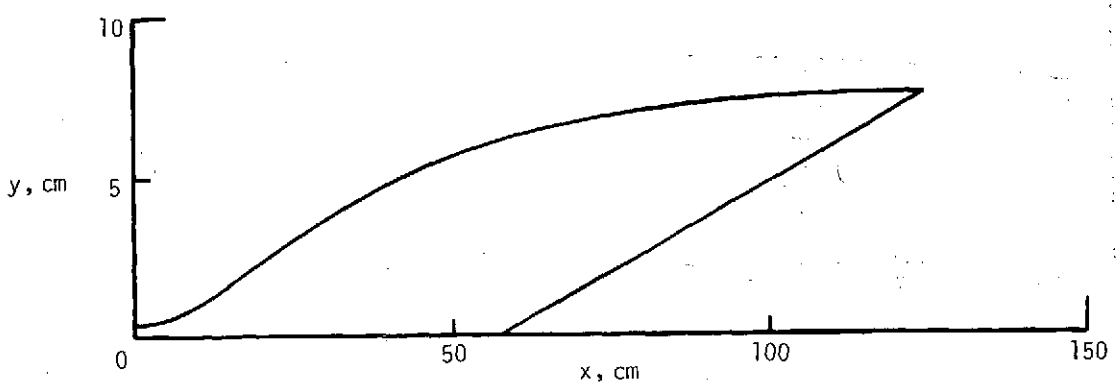

Figure 13.- Nozzle contour for the vibrational sudden-freeze model. p_t = 100 atm; T_t = 3400 K; $M_\infty \approx 9$.

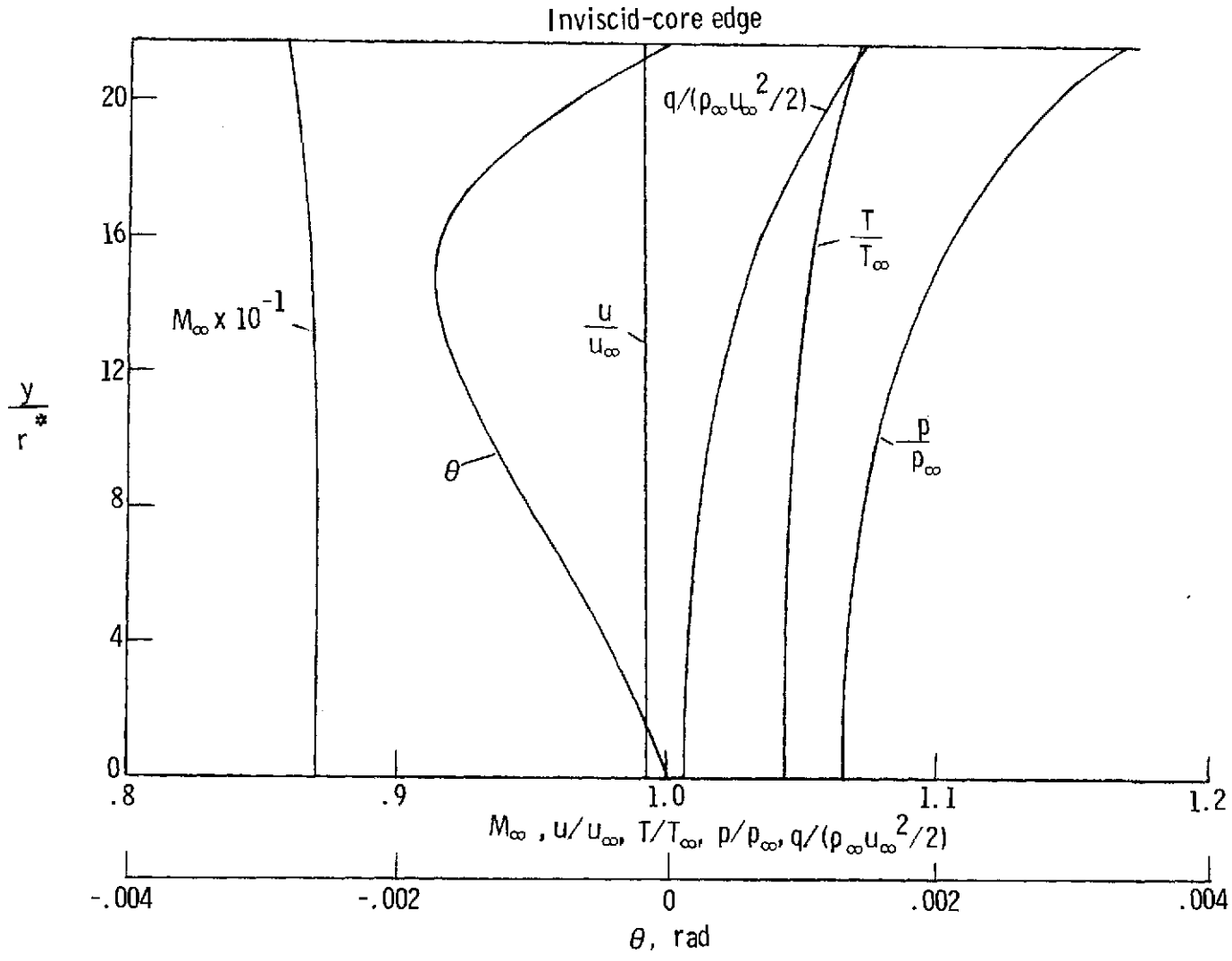

Figure 14.- Exit profiles for sudden-freeze nozzle design. $r^* = 0.350$ cm; $p_t = 100$ atm; $T_t = 3400$ K.

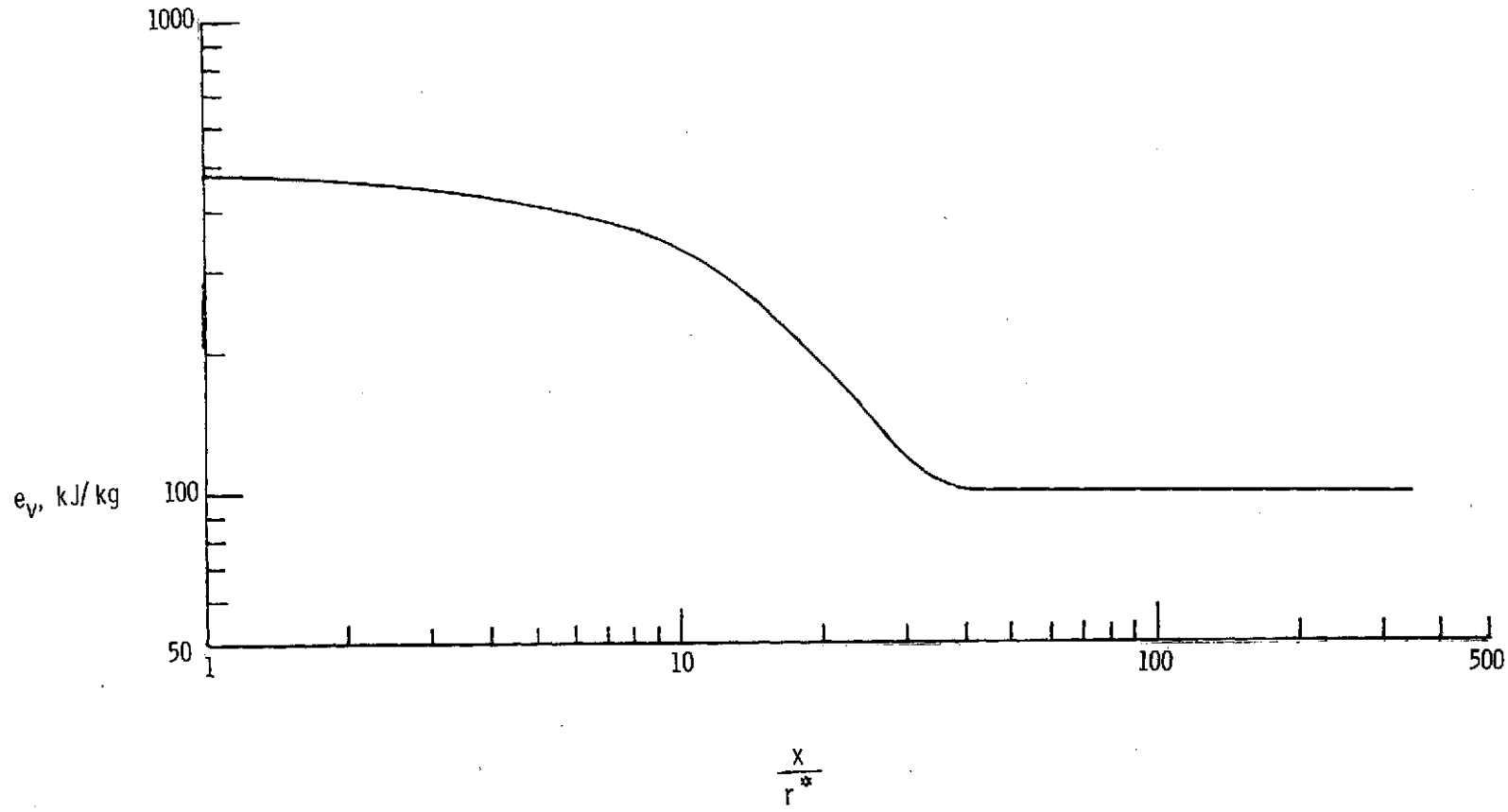

Figure 15.- Energy in vibration along nozzle center line. $r^* = 0.350$ cm; $p_t = 100$ atm; $T_t = 3400$ K.

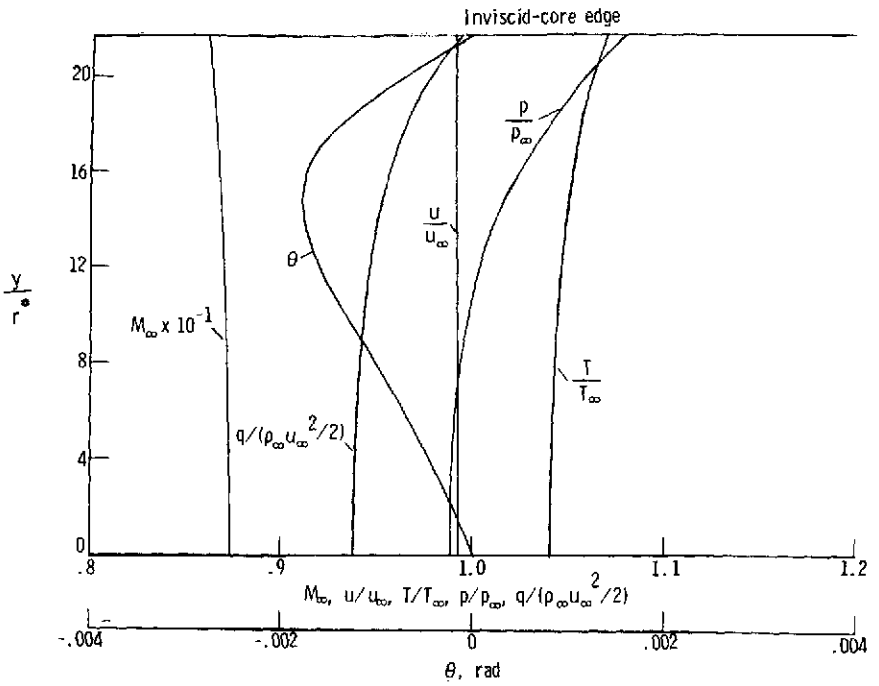

(a) p_t = 90 atm; T_t = 3400 K.

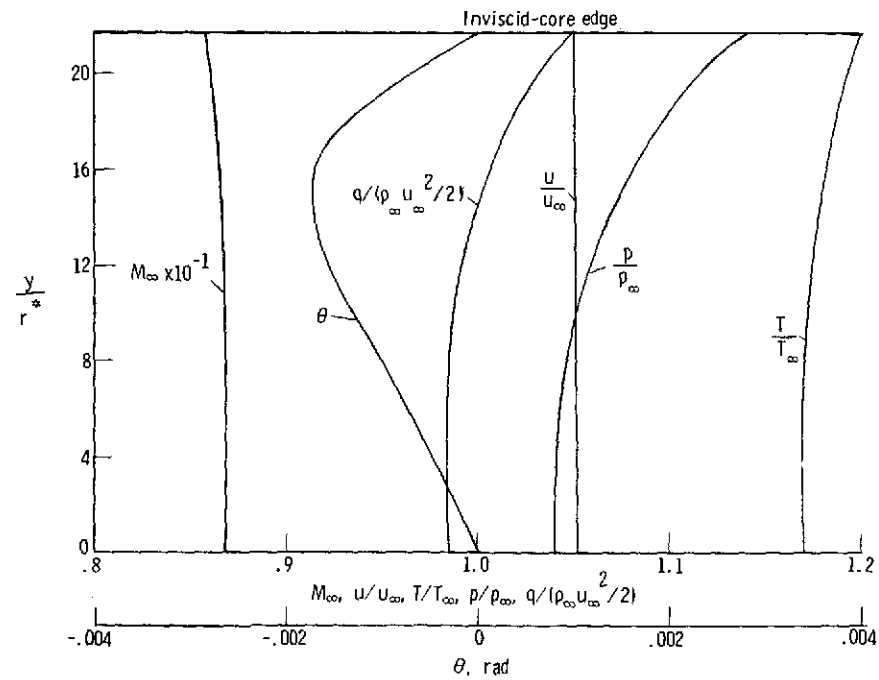

(b) p_t = 100 atm; T_t = 3740 K.

Figure 16.- Exit profiles for off-design conditions. r^* = 0.350 cm.

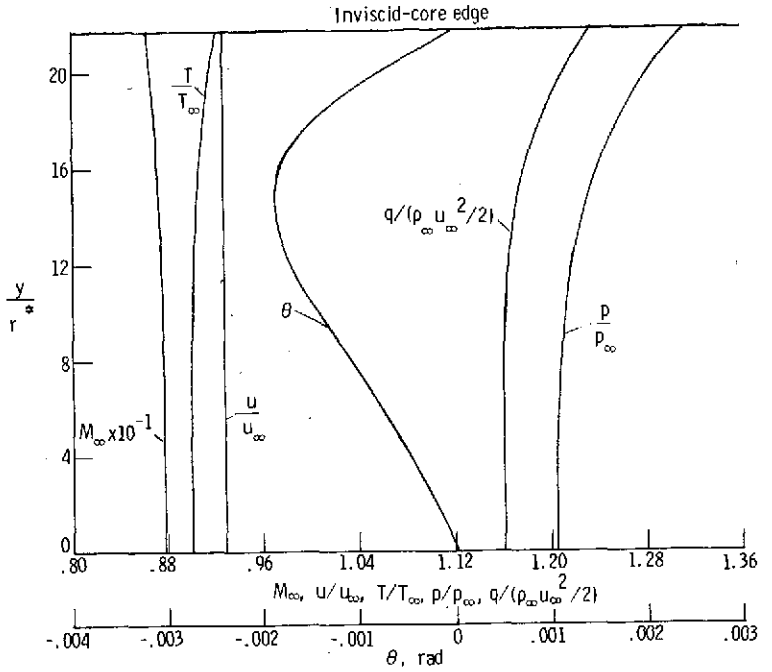

(c) p_t = 90 atm; T_t = 3000 K.

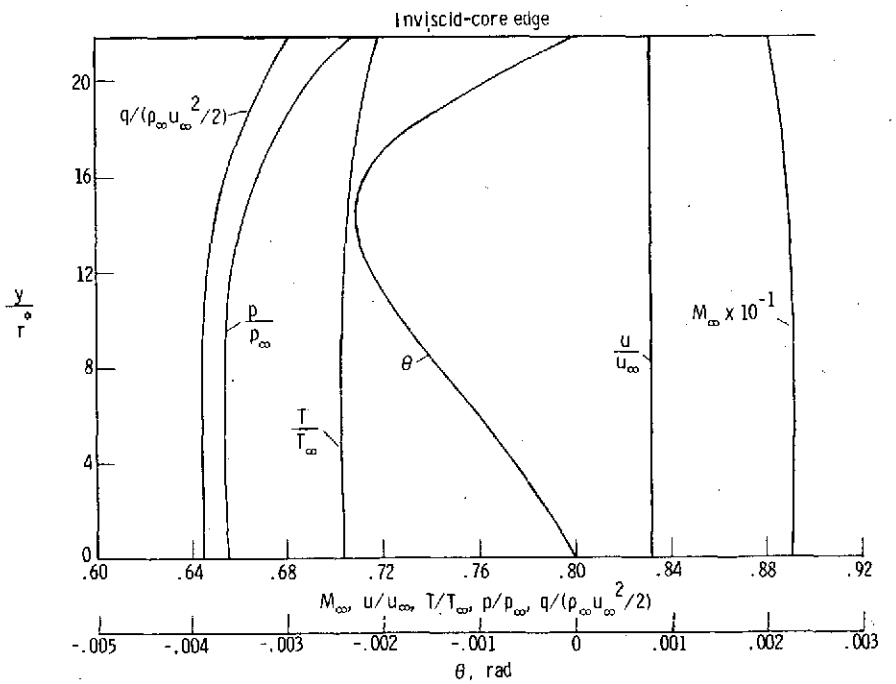

(c) p_t = 65 atm; T_t = 2500 K.

Figure 16.- Concluded.